Office of Naval Research

Contract Nonr-1866(49)

NR - 015 - 807

ARPA Order No. 455

FINAL TECHNICAL REPORT

Covering Period June 1, 1963 - June 1, 1965

The research reported in this document was made possible through support extended the Division of Engineering and Applied Physics, Harvard University, by Project DEFENDER under the joint sponsorship of the Advanced Research Projects Agency, Department of Defense and the Office of Naval Research, Department of the Navy.

Submitted by:

N. Bloembergen, Project Director

Cruft Laboratory

Division of Engineering and Applied Physics

Harvard University

Cambridge, Massachusetts

FINAL TECHNICAL REPORT

Covering Period June 1, 1963 - June 1, 1965

FOREWORD

This report constitutes the Final Report performed under contract Nonr 1866(49) at the Gordon McKay Laboratory. The research carried out for Project DEFENDER was concerned with the Optical Properties of Materials at Very High Light Intensities. This work is closely related to research carried out in the general field of Nonlinear Optics supported under the continuing contracts Nonr 1866(28) and Nonr 1866(16). Some of the research reported here received joint support under the three contracts. This Final Report reviews the entire period of the contract Nonr 1866(49), but more specifically the period from June 1, 1964, through June 1, 1965. The following personnel has been associated with the project during the final year:

Professor N. Bloembergen	Project Director and Principal Investigator
Dr. J. Ducuing	Research Fellow
Dr. R. K. Chang	Graduate Student
Mr. P. Lallemand	Graduate Student

In the previous period, Dr. J. van der Ziel, research fellow, and Mr. L. Malmstrom, a graduate student, have also been associated with the project.

Since all essential results obtained under this contract have already been reported in the published literature, this Final Report consists only of a Summary to which the reprints of published papers are attached as appendices. Related papers, which did not receive support under contract Nonr 1866(49), have not been included.

SUMMARY

The two major experimental efforts partially supported by this contract were concerned with A) The second harmonic production of light in semiconductors and B) The stimulated Raman effect in liquids.

A) The complex nonlinear susceptibility describing the second harmonic generation of light in semiconducting III-V and II-VI compounds has been measured as a function of frequency. Both the real and imaginary parts have been determined. The determination of the phase of the complex susceptibility has been accomplished for the first time. This novel method is described in Appendix I. Another new result is the variation of the nonlinear susceptibility as a function of frequency in the same sample. The experimental results are shown in Appendix II. Further experimental and theoretical investigations in this new field of nonlinear spectroscopy of solids will be carried out under other contracts.

B) A Raman amplifier cell technique has been developed to give a more reliable determination of the stimulated Raman gain in fluids. This method is described in Appendix III. The work in Appendix IV was presented at the International Conference on the Physics of Quantum Electronics, held in June 1965, in San Juan (P. R.). The most striking result is that the gain per unit length in a cell filled with Raman fluid changes as the laser beam progresses into the medium.

Furthermore, the initial gain per unit length depends on the distance of separation between the Raman laser oscillator and the amplifier cell. Subsequent work with the same equipment has shown that the intensity distribution in the laser beam changes as it traverses through the fluid. Experiments with different fluids in two Raman cells in series have demonstrated that this effect is due to self-focusing of the laser beam. There is a transverse gradient in the index of refraction, because this index is dependent on the intensity. The self-focusing effect is entirely distinct and separable from the stimulated Raman effect. It is most pronounced in fluids with anisotropic molecules and is well correlated with the anisotropy in the optical polarizability of these molecules. The effect is described in Appendix V. The discrepancies of one or two orders of magnitude in the experimental and theoretical values of the Raman gain in certain fluids are thus largely explained by the creation of filaments of high intensity in the laser beam due to self-focusing. These experiments have obviously important consequences for the design of Raman lasers and the passage of high intensity laser beams through media with anisotropic molecules. Further experimental work on factors determining the size and distribution of the bright filaments, on the influence of focusing on the stimulated Brillouin effect, on the magnitude of focusing effects and Raman gain in fluids with isotropic molecules, etc., is obviously suggested and will be carried out under other contracts.

APPENDIX 1

RELATIVE PHASE MEASUREMENT BETWEEN FUNDAMENTAL AND SECOND-HARMONIC LIGHT*

R. K. Chang
Gordon McKay Laboratory, Harvard University, Cambridge, Massachusetts

J. Ducuing
Physics Department, Massachusetts Institute of Technology, Cambridge, Massachusetts

N. Bloembergen†
Departments of Electrical Engineering and Physics, University of California, Berkeley, California
(Received 14 June 1965)

The nonlinear susceptibility describing the second-harmonic generation of light is real, when the medium is transparent at both the fundamental and the harmonic frequency. When the medium is absorbing at either or both of these frequencies, this nonlinear susceptibility is a complex quantity.[1] The nonlinear polarization has a phase shift with respect to the fundamental field. Measurement of the second-harmonic intensity only determines the absolute value of the nonlinear susceptibility. For some III-V and II-VI compounds, which are absorbing at the second-harmonic frequency, such measurements have been carried out in reflection.[2,3] In this note an experiment is described which determines the phase of the nonlinear susceptibility.

The experimental arrangement is shown in Fig. 1. A linear polarized laser beam from a Q-switched ruby laser enters an evacuated box and generates second-harmonic radiation by reflection from a nonlinear mirror of a crystal with $\bar{4}3m$ symmetry, whose complex nonlinear susceptibility must be determined. The laser beam subsequently generates an additional second-harmonic field in a potassium-dihydrogen-phosphate (KDP) platelet which serves as a reference signal. The second-harmonic fields generated in the two samples will have a definite phase relationship with respect to each other, as each has a specific relationship to the phase of the fundamental

L561 1-3

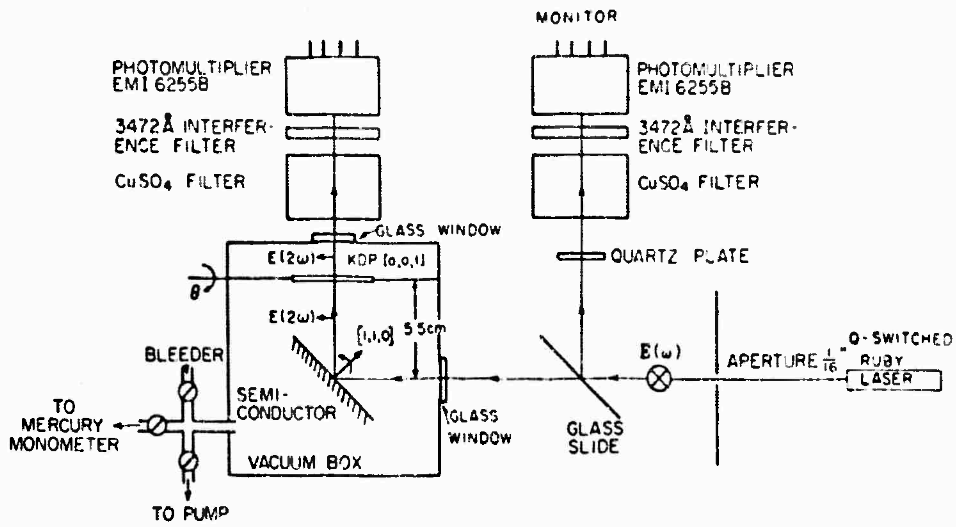

FIG. 1. Diagram of the experimental apparatus to determine the relative phase of the second-harmonic field, as described in the text. Each laser pulse is monitored by the harmonic production in quartz.

field squared. The total second-harmonic output is the result of the interference between the two second-harmonic beams. This interference can be made visible by admitting dry air into the box. The dispersion in air changes the relative phase between the fundamental and second harmonic in the 5.5-cm path between the reflection spot on the mirror and the KDP crystal. From tabulated dispersion data for air, a phase shift of 180° occurs for an air pressure equivalent to 22 cm Hg. The second-harmonic intensity emerging from the box is shown in Fig. 2 as a function of air pressure. It has the expected periodicity.

The KDP platelet is a (100) cut, and can be tilted around the (001) direction. The polarization of the laser beam is almost parallel to the (010) direction. In this manner the second-harmonic production in the platelet may be kept very small and made comparable to, but slightly larger than, the second-harmonic production in the mirror.

The nonlinear mirror may be turned around its (110) normal so that the laser field points along the (001) cubic axis. In this case no second harmonic is generated in the mirror.[4] The KDP platelet is then tilted, so that its second-harmonic output is a relative maximum.

Next the mirror is turned so that the fundamental field points along the (110) direction. The mirror then produces a second-harmonic field parallel to that generated in the KDP crystal. The interference pattern in Fig. 2 is observed, when the air pressure in the cell is increased. If the fundamental field points along the (111) direction of the crystal mirror, no

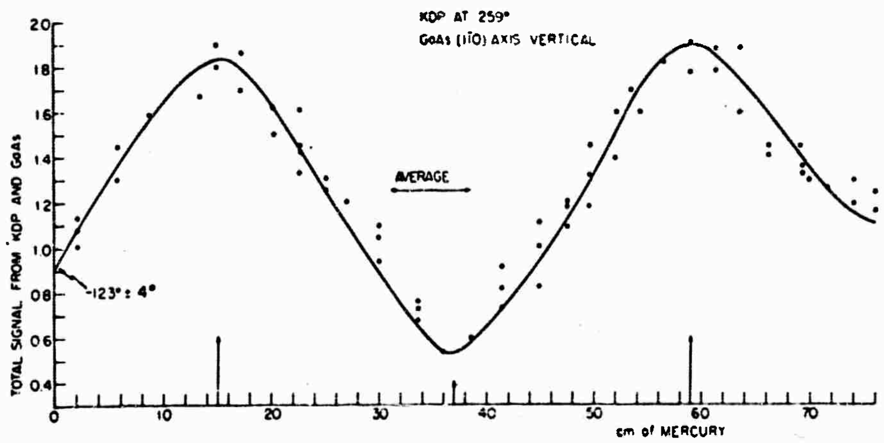

FIG. 2. The interference between the second-harmonic fields produced by the same laser beam in the GaAs mirror and the KDP platelet, as a function of the air pressure in the box shown in Fig. 1.

L561 2-3

interference is observed because in this case the fields generated in the two samples are orthogonal.

The position of the first extremum in Fig. 2 is a measure for the phase relationship between the squared fundamental field and the second-harmonic field after reflection from the nonlinear mirror. From the angles for which zero harmonic production occurs in KDP, one can determine exactly the phase shift $\delta\varphi_{KDP}$ of the harmonic generated in KDP with respect to that of the harmonic from the nonlinear mirror. For our particular case $\delta\varphi_{KDP} = (\pi + 13°30')$ $\pm 3°30'$ when the KDP is tilted so that its second-harmonic output is a relative maximum.

The sign of the interference is reversed if either the $\bar{4}3m$ crystal or the KDP crystal is replaced by its piezoelectric antipode, or inversion image. All phases in the following discussion have therefore an ambiguity of 180°. This ambiguity of sign can only be eliminated if the sign of the piezoelectric tensor is measured and related to the absolute structure, both for KDP and the $\bar{4}3m$ crystals.

The experimental phase shift Δ between the position for zero pressure and the first extremum can be determined from Fig. 2 to be $-123° \pm 4°(+180°)$ for GaAs. For a mirror of InAs this phase angle was found to be $-90°$ $\pm 4°(+180°)$ and for ZnTe $0° \pm 4°(+180°)$. From these observations the phase angle φ_{NL} of the complex nonlinear susceptibility may be calculated from the relation

$$\Delta = \varphi_{NL} + \varphi(2\omega) - 2\varphi(\omega) - \delta\varphi_{KDP}. \tag{1}$$

The phase angle $\varphi(\omega)$ is the phase shift on reflection of the fundamental field, determined by the Fresnel formula for 45° angle of incidence,

$$\frac{E_R(\omega)}{E_i(\omega)} = \frac{1-\alpha(\omega)}{1+\alpha(\omega)} = r_1 e^{i\varphi(\omega)}, \tag{2}$$

where

$$\alpha(\omega) = \{2\epsilon(\omega) - 1\}^{1/2}.$$

The phase angle $\varphi(2\omega)$ follows from the nonlinear laws of reflection,[5] which for the geometry of Fig. 1 may be written in the form

$$E_R(2\omega) = E_i^{\,2}(\omega)|\chi^{NL}|\exp(i\varphi_{NL})r_2 e^{i\varphi(2\omega)},$$

with

$$r_2 e^{i\varphi(2\omega)}$$

$$= \frac{32\pi}{\sqrt{2}} \frac{\alpha(2\omega)}{\{\alpha(\omega)+1\}^2\{\alpha(2\omega)+1\}^2\{\alpha(\omega)+\alpha(2\omega)\}}. \tag{3}$$

When the known values of the complex dielectric constants are inserted in Eqs. (1)-(3), the following phase angles for the nonlinear susceptibility are found: $\varphi_{NL} = -71° \pm 19°(+180°)$ for GaAs, $\varphi_{NL} = -37° \pm 20°(+180°)$ for InAs, and $\varphi_{NL} = 34° \pm 24°(+180°)$ for ZnTe. With the previously measured second-harmonic intensities[2,3] the estimated nonlinear susceptibilities relative to KDP become

$$\chi_{GaAs}^{NL}/\chi_{KDP} = \pm(165 - 475i),$$

$$\chi_{InAs}^{NL}/\chi_{KDP} = \pm(272 - 204i),$$

and

$$\chi_{ZnTe}/\chi_{KDP} = \pm(552 + 372i).$$

---

*This research was supported by the Joint Services Electronics Program under contract Nonr 1866 (16).

†On leave from Harvard University.

[1]N. Bloembergen, Proc. IEEE 51, 124 (1963).

[2]N. Bloembergen, R. K. Chang, J. Ducuing, and P. Lallemand, Proceedings of the International Conference on Semiconductors, Paris, 1964 (Academic Press, Inc., New York, 1964).

[3]R. K. Chang, J. Ducuing, and N. Bloembergen (unpublished).

[4]J. Ducuing and N. Bloembergen, Phys. Rev. Letters 10, 474 (1963).

[5]N. Bloembergen and P. S. Pershan, Phys. Rev. 128, 606 (1962). Especially Eq. 4.13 of this paper is used with $\alpha + \theta_S = \pi/2$ and $\theta_R = \pi/4$.

L561 3-3

APPENDIX 2

DISPERSION OF THE OPTICAL NONLINEARITY IN SEMICONDUCTORS*

R. K. Chang

Gordon McKay Laboratory, Harvard University, Cambridge, Massachusetts

and

J. Ducuing

Physics Department, Massachusetts Institute of Technology, Cambridge, Massachusetts

and

N. Bloembergen†

Department of Electrical Engineering and Physics, University of California, Berkeley, California

(Received 8 June 1965)

The dispersion of the modulus of the nonlinear susceptibility $\chi_{14}^{NL}(2\omega)$ (where NL stands for nonlinear) responsible for second-harmonic (SH) generation has been directly measured for the first time. The crystals investigated were several semiconductors having zincblende ($\bar{4}3m$) symmetry. The frequency range not only includes the absorption-edge region, but also extends well inside this region. A rapid variation of $|\chi_{14}^{NL}(2\omega)|$ as a function of frequency is observed. Pronounced maxima can be correlated with the presence of the critical points in the joint density of states in the vicinity of the fundamental and/or harmonic photon energy. Such correlations are similar to the ones found in the linear optical data.[1,2] In addition, the nonlinear susceptibility, which is zero when the crystal has inversion symmetry, depends on the antisymmetric potential[3] which mixes the wave functions of different parity. This then leads to marked differences between the linear and nonlinear cases.

Nine different fundamental sources having photon energies in the range from 1.17 to 2.34 eV were used. The lowest photon energy is that of a Nd-doped glass laser, the highest that of its harmonic obtained by prior frequency doubling in a KDP crystal. The other frequencies are those of a ruby laser and its Stokes lines obtained by stimulated scattering from various fluids: H_2 gas gives a Stokes energy of 1.27 eV, cyclohexane 1.43 eV: benzene gives a first Stokes energy at 1.66 eV and a second Stokes at 1.54 eV; nitrobenzene gives a Stokes line at 1.62 eV; and CS_2 at 1.70 eV.

The experimental arrangement is shown in Fig. 1. The nonlinear susceptibility of single crystals was measured by the method of reflected harmonics.[4] Second-harmonic production in a quartz plate is used to monitor the

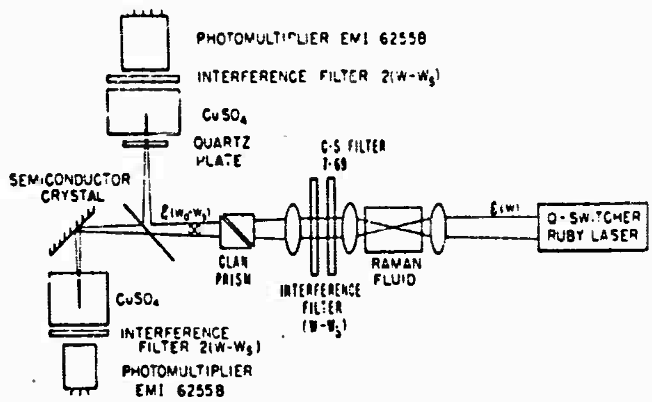

FIG. 1. Diagram of the experimental arrangement for the case when the incident radiation is produced by stimulated Raman scattering.

laser intensity.[5] The intensity of the reflected harmonic beam from the semiconductor is measured and compared to that produced in transmission through a KDP crystal by the same source.[6] The nonlinear susceptibility of KDP is assumed to be independent of frequency in this range and taken as a reference.

The nonlinear second-order sysceptibility tensor for a crystal with $\bar{4}3m$ symmetry has only three elements different from zero: $\chi_{14}^{NL}(2\omega)=\chi_{25}^{NL}(2\omega)=\chi_{36}^{NL}(2\omega)$. An expression for the nonlinearity appropriate for a semiconductor has been derived.[7,8] A straightforward rearrangement of this expression yields

$$\chi_{14}^{NL}(2\omega)=A \lim_{\mathrm{Im}\,\omega\to 0}\sum_{l,l'}\int_{BZ} d^3k\, f(E_{l,k})$$

$$\times\left\{\frac{Q_{ll'}^{(1)}(k)}{\omega^2-\omega_{ll'}^{\;2}}+\frac{Q_{ll'}^{(2)}(k)}{4\omega^2-\omega_{ll'}^{\;2}}\right\}, \qquad (1)$$

where A is frequency independent, $f(E_{l,k})$ is

interference is observed because in this case the fields generated in the two samples are orthogonal.

The position of the first extremum in Fig. 2 is a measure for the phase relationship between the squared fundamental field and the second-harmonic field after reflection from the nonlinear mirror. From the angles for which zero harmonic production occurs in KDP, one can determine exactly the phase shift $\delta\varphi_{KDP}$ of the harmonic generated in KDP with respect to that of the harmonic from the nonlinear mirror. For our particular case $\delta\varphi_{KDP} = (\pi + 13°30') \pm 3°30'$ when the KDP is tilted so that its second-harmonic output is a relative maximum.

The sign of the interference is reversed if either the $\bar{4}3m$ crystal or the KDP crystal is replaced by its piezoelectric antipode, or inversion image. All phases in the following discussion have therefore an ambiguity of 180°. This ambiguity of sign can only be eliminated if the sign of the piezoelectric tensor is measured and related to the absolute structure, both for KDP and the $\bar{4}3m$ crystals.

The experimental phase shift Δ between the position for zero pressure and the first extremum can be determined from Fig. 2 to be $-123° \pm 4°(+180°)$ for GaAs. For a mirror of InAs this phase angle was found to be $-90° \pm 4°(+180°)$ and for ZnTe $0° \pm 4°(+180°)$. From these observations the phase angle φ_{NL} of the complex nonlinear susceptibility may be calculated from the relation

$$\Delta = \varphi_{NL} + \varphi(2\omega) - 2\varphi(\omega) - \delta\varphi_{KDP}. \quad (1)$$

The phase angle $\varphi(\omega)$ is the phase shift on reflection of the fundamental field, determined by the Fresnel formula for 45° angle of incidence,

$$\frac{E_R(\omega)}{E_i(\omega)} = \frac{1-\alpha(\omega)}{1+\alpha(\omega)} = r_1 e^{i\varphi(\omega)}, \quad (2)$$

where

$$\alpha(\omega) = \{2\epsilon(\omega) - 1\}^{1/2}.$$

The phase angle $\varphi(2\omega)$ follows from the nonlinear laws of reflection,[5] which for the geometry of Fig. 1 may be written in the form

$$E_R(2\omega) = E_i^2(\omega)|\chi^{NL}|\exp(i\varphi_{NL}) r_2 e^{i\varphi(2\omega)},$$

with

$$r_2 e^{i\varphi(2\omega)} = \frac{32\pi}{\sqrt{2}} \frac{\alpha(2\omega)}{\{\alpha(\omega)+1\}^2\{\alpha(2\omega)+1\}^2\{\alpha(\omega)+\alpha(2\omega)\}}. \quad (3)$$

When the known values of the complex dielectric constants are inserted in Eqs. (1)-(3), the following phase angles for the nonlinear susceptibility are found: $\varphi_{NL} = -71° \pm 19°(+180°)$ for GaAs, $\varphi_{NL} = -37° \pm 20°(+180°)$ for InAs, and $\varphi_{NL} = 34° \pm 24°(+180°)$ for ZnTe. With the previously measured second-harmonic intensities[2,3] the estimated nonlinear susceptibilities relative to KDP become

$$\chi_{GaAs}^{NL}/\chi_{KDP} = \pm(165 - 475i),$$

$$\chi_{InAs}^{NL}/\chi_{KDP} = \pm(272 - 204i),$$

and

$$\chi_{ZnTe}/\chi_{KDP} = \pm(552 + 372i).$$

---

*This research was supported by the Joint Services Electronics Program under contract Nonr 1866 (16).

†On leave from Harvard University.

[1]N. Bloembergen, Proc. IEEE 51, 124 (1963).

[2]N. Bloembergen, R. K. Chang, J. Ducuing, and P. Lallemand, Proceedings of the International Conference on Semiconductors, Paris, 1964 (Academic Press, Inc., New York, 1964).

[3]R. K. Chang, J. Ducuing, and N. Bloembergen (unpublished).

[4]J. Ducuing and N. Bloembergen, Phys. Rev. Letters 10, 474 (1963).

[5]N. Bloembergen and P. S. Pershan, Phys. Rev. 128, 606 (1962). Especially Eq. 4.13 of this paper is used with $\alpha + \theta_S = \pi/2$ and $\theta_R = \pi/4$.

APPENDIX 2

DISPERSION OF THE OPTICAL NONLINEARITY IN SEMICONDUCTORS*

R. K. Chang

Gordon McKay Laboratory, Harvard University, Cambridge, Massachusetts

and

J. Ducuing

Physics Department, Massachusetts Institute of Technology, Cambridge, Massachusetts

and

N. Bloembergen†

Department of Electrical Engineering and Physics, University of California, Berkeley, California

(Received 8 June 1965)

The dispersion of the modulus of the nonlinear susceptibility $\chi_{14}^{NL}(2\omega)$ (where NL stands for nonlinear) responsible for second-harmonic (SH) generation has been directly measured for the first time. The crystals investigated were several semiconductors having zincblende ($\bar{4}3m$) symmetry. The frequency range not only includes the absorption-edge region, but also extends well inside this region. A rapid variation of $|\chi_{14}^{NL}(2\omega)|$ as a function of frequency is observed. Pronounced maxima can be correlated with the presence of the critical points in the joint density of states in the vicinity of the fundamental and/or harmonic photon energy. Such correlations are similar to the ones found in the linear optical data.[1,2] In addition, the nonlinear susceptibility, which is zero when the crystal has inversion symmetry, depends on the antisymmetric potential[3] which mixes the wave functions of different parity. This then leads to marked differences between the linear and nonlinear cases.

Nine different fundamental sources having photon energies in the range from 1.17 to 2.34 eV were used. The lowest photon energy is that of a Nd-doped glass laser, the highest that of its harmonic obtained by prior frequency doubling in a KDP crystal. The other frequencies are those of a ruby laser and its Stokes lines obtained by stimulated scattering from various fluids: H_2 gas gives a Stokes energy of 1.27 eV, cyclohexane 1.43 eV; benzene gives a first Stokes energy at 1.66 eV and a second Stokes at 1.54 eV; nitrobenzene gives a Stokes line at 1.62 eV; and CS_2 at 1.70 eV.

The experimental arrangement is shown in Fig. 1. The nonlinear susceptibility of single crystals was measured by the method of reflected harmonics.[4] Second-harmonic production in a quartz plate is used to monitor the laser intensity.[5] The intensity of the reflected harmonic beam from the semiconductor is measured and compared to that produced in transmission through a KDP crystal by the same source.[6] The nonlinear susceptibility of KDP is assumed to be independent of frequency in this range and taken as a reference.

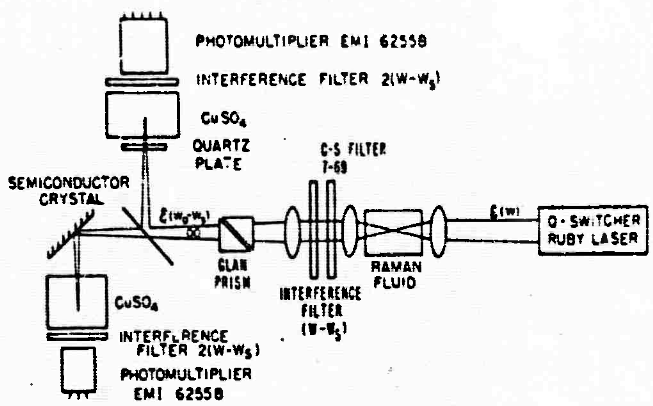

FIG. 1. Diagram of the experimental arrangement for the case when the incident radiation is produced by stimulated Raman scattering.

The nonlinear second-order susceptibility tensor for a crystal with $\bar{4}3m$ symmetry has only three elements different from zero: $\chi_{14}^{NL}(2\omega)=\chi_{25}^{NL}(2\omega)=\chi_{36}^{NL}(2\omega)$. An expression for the nonlinearity appropriate for a semiconductor has been derived.[7,8] A straightforward rearrangement of this expression yields

$$\chi_{14}^{NL}(2\omega)=A \lim_{\mathrm{Im}\,\omega\to 0}\sum_{l,l'}\int_{BZ} d^3k\, f(E_{l,k}) \times\left\{\frac{Q_{ll'}^{(1)}(k)}{\omega^2-\omega_{ll'}^2}+\frac{Q_{ll'}^{(2)}(k)}{4\omega^2-\omega_{ll'}^2}\right\}, \quad (1)$$

where A is frequency independent, $f(E_{l,k})$ is

L545 1-4

the Fermi-Dirac distribution function giving the occupation number of the state with the energy $E_{l,k}$. The summation is over band indexes, and the integration extends over the Brillouin zone (BZ). The quantities $Q_{ll'}(k)$ which involve a summation over intermediate states are real and independent of frequency. They vanish for a material possessing inversion symmetry. The above expression is to be compared with the corresponding one for the linear susceptibility

$$\chi^{L}(2\omega)=B \lim_{\mathrm{Im}\omega\to 0} \sum_{l,l'} \int_{BZ} d^3k f(E_{l,k}) \times \frac{|P_{ll'}(k)|^2}{\omega_{ll'}} \frac{1}{4\omega^2-\omega_{ll'}^2}, \quad (2)$$

where B is also independent of frequency, the $P_{ll'}(k)$ are suitable reduced-momentum matrix elements,[2] and L stands for linear. The $|P_{ll'}(k)|^2$ are known to be slowly varying functions of k.[9] Were this to be also true of the quantities $Q_{ll'}(k)$, the dispersion of $\chi^{NL}(2\omega)$ would be almost entirely governed by the joint density of states between bands l, l', as is the case for χ^{L}. If the contribution from the highest valence band and the lowest conduction band is dominant, as in the case of χ^{L}, the nonlinear susceptibility could then be represented to an excellent approximation by a linear combination of the values $\chi^{L}(\omega)$ and $\chi^{L}(2\omega)$. In general, such a relation will not hold, as the coefficients $Q_{ll'}(k)$, which involve triple products of the reduced-momentum matrix elements, depend on the phase of these latter quantities. The Q's can vary appreciably over the Brillouin zone, changing in sign as well as in magnitude. Because of this, the dispersion of χ^{NL} will not be determined entirely by the joint density of states. There may also appear additional structure due to the variation of the $Q_{ll'}(k)$ over the Brillouin zone.

The experimental error brackets stem from two causes. First, there is a consistent error of ±10% in determining the ratio of intensity of the reflected SH from the semiconductor and the intensity of the SH from KDP by transmission. The second source of error, which for many cases is the larger of the two, results from not being able to determine exactly the real and imaginary part of the linear dielectric constant, especially when one or both of them are sharply peaked. The Fresnel factors for nonlinear reflectors are a sensitive function of them. The values of the linear dielectric constant for GaAs, InAs, and InSb were obtained from Philipp and Ehrenreich.[2] For ZnTe, a Kramers-Kronig transform was performed using the available data on reflectivity and suitable extrapolation for the high-energy region.[10-12]

The case of ZnTe [Fig. 2(a)] provides a striking illustration of the variation of $|\chi_{14}^{NL}(2\omega)|$ when the harmonic photon energy penetrates progressively inside the absorption region. Over the investigated range the absorption of the fundamental is negligible, but that of the harmonic increases by more than an order of magnitude to reach a maximum around $2\omega = 3.6$ eV, which corresponds to the peak called E_1 in semiconductor terminology in the joint density of states. Under these circumstances the second term inside the brackets in Eq. (1) ought to predominate entirely; that is, the density of states at $2\hbar\omega$ governs the behavior of $|\chi_{14}^{NL}(2\omega)|$. Experimentally, as $2\hbar\omega$ penetrates inside the absorption band, $|\chi_{14}^{NL}(2\omega)|$ increases progressively. Soref and Moos[13] had previously observed a similar behavior at a fixed light frequency when the band gap was varied in (ZnCd) S alloys. However, as they pointed out, their method assumes that the properties of the semiconductor-alloy series are such that varying the band gap by alloying is equivalent to shifting the applied laser frequency.

A different situation exists in InSb [Fig. 2(b)]. Here both the harmonic and fundamental photon energy are absorbed. As the source frequency increases, the fundamental photon energy $\hbar\omega$ gets closer to the E_1 peak, which for InSb appears at a much lower value (1.83 eV) than for ZnTe. On the other hand, there exists no critical point of the joint density of states within the interval covered by the harmonic photon energy, as evidenced by the fact that $\chi^{L}(2\omega)$ has no pronounced structure. This should result in a strong influence of the first term in Eq. (1) on the dispersion of $\chi^{NL}(2\omega)$. A pronounced variation of $|\chi_{14}^{NL}(2\omega)|$ is observed experimentally, which seems to be somewhat related to that of the real part of the linear susceptibility $\chi^{L}(\omega)$. The maximum value appears at $\hbar\omega = 1.6$ eV, where the $|\chi_{14}^{NL}(2\omega)| = 5\times10^{-6}$ esu. This is the highest value measured for a second-order susceptibility, nearly 2000 times higher than the corresponding value for KDP.

For GaAs [Fig. 2(c)], the E_1 peak again appears at higher value (2.90 eV), and the main

L545 2-4

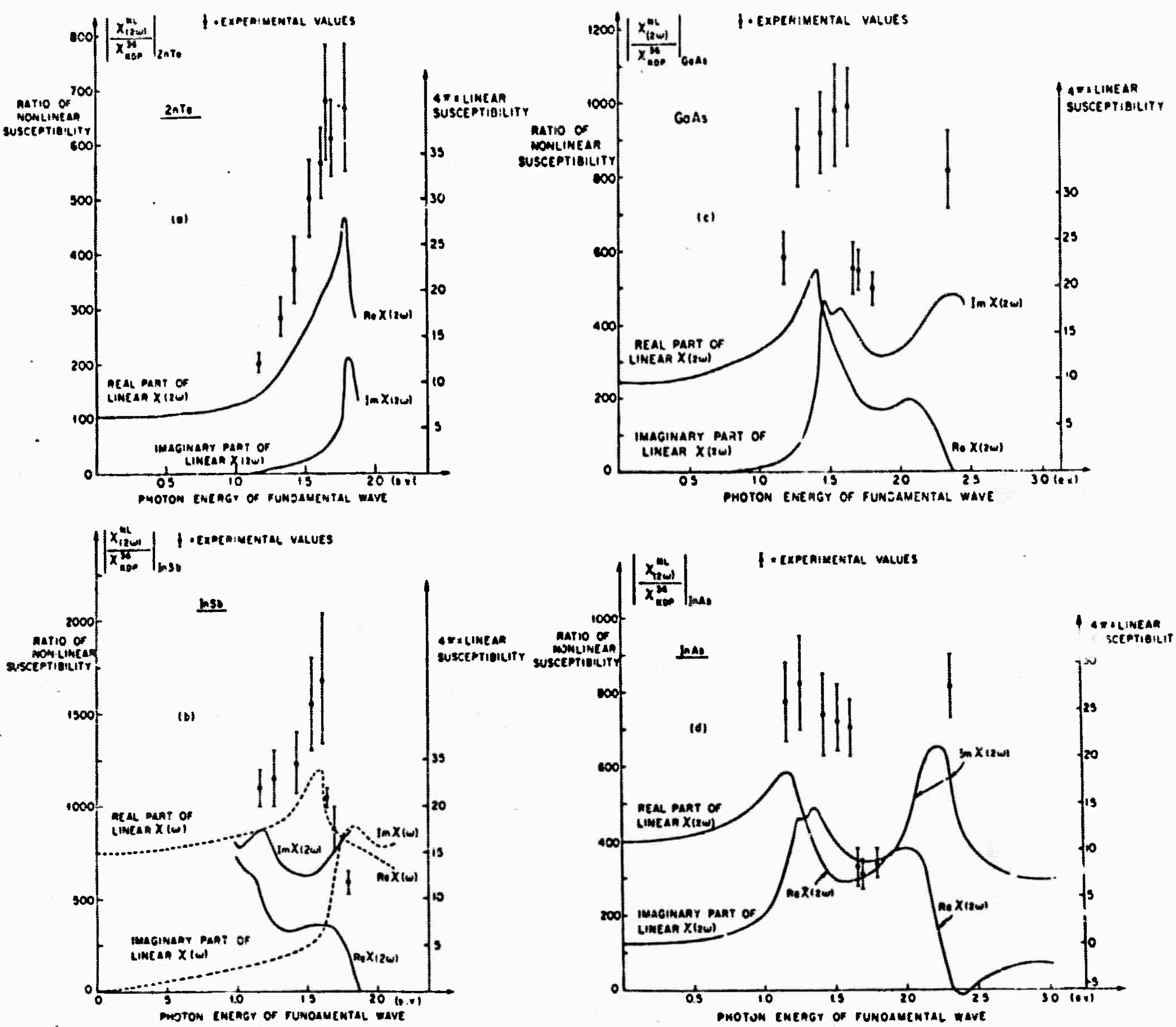

FIG. 2. The modulus $|\chi_{14}^{NL}(2\omega)|$ of the nonlinear susceptibility of (a) ZnTe; (b) InSb; (c) GaAs; and (d) InAs. The bar indicates the maximum uncertainty resulting from various sources of error. For the sake of comparison, the real and imaginary parts of the linear susceptibility $\chi^L(2\omega)$ have been plotted in all cases, while those of $\chi^L(\omega)$ are also displayed in case (b).

features of the dispersion are given by the second term in Eq. (1). Here a pronounced peak in $|\chi_{14}^{NL}(2\omega)|$ also exists in the neighborhood of the E_1 peak. Two novel features appear in the results for GaAs. First, at the highest source frequency, the harmonic photon energy is near the E_2 peak $(X_{5v}-X_{3c},X_{1c})$. A corresponding increase in the nonlinearity is observed. The contribution from the first term of Eq. (1) might also be significant at this point. Second, a very sharp decrease in $|\chi_{14}^{NL}(2\omega)|$ is observed around 1.67 eV. As seen from the linear data, the joint density of states does not exhibit such a fast variation and thus cannot be held responsible for this sharp decrease. Such data must probably be accounted for by a pronounced structure in the Q's. InAs [Fig. 2(d)] yields, as expected, results very similar to those obtained for GaAs. Both these features were observed again.

Our dispersion results clearly show the influence of the critical points in the density of states. They also bring out some features related to the Q's and hence to the hybridization of the wave function. The dispersion of the real and imaginary[14] part of $|\chi^{NL}(2\omega)|$ should provide some information not available from the study of linear properties alone.

---

*This research was supported by the Joint Services

Electronics Program under Contract No. NONR 1866-16, Harvard University.

†On leave from Harvard University, Cambridge, Massachusetts.

[1]D. Brust, J. C. Phillips, and F. Bassani, Phys. Rev. Letters 9, 94 (1962).

[2]H. R. Philipp and H. Ehrenreich, Phys. Rev. 129, 1550 (1962).

[3]F. J. Herman, Electronics 1, 103 (1955).

[4]J. Ducuing and N. Bloembergen, Phys. Rev. Letters 10, 474 (1963).

[5]J. Ducuing and N. Bloembergen, Phys. Rev., 133 A1473 (1964).

[6]N. Bloembergen, R. K. Chang, J. Ducuing, and P. Lallemand, in Proceedings of the Seventh International Conference on Simiconductors (Dunod, Paris, 1964).

[7]P. N. Butcher and T. P. McLean, Proc. Phys. Soc. (London) 81, 219 (1963).

[8]P. L. Kelley, J. Phys. Chem. Solids 24, 607, 1113 (1963).

[9]D. Brust, Phys. Rev. 134, A1337 (1964).

[10]D. T. F. Marple, J. Appl. Phys. 35, 539 (1964).

[11]M. Cardona and S. Greenway, Phys. Rev. 131, 98 (1963).

[12]F. Stern, Solid State Phys. 15, 300 (1964).

[13]R. A. Soref and H. W. Moos, J. Appl. Phys. 35, 2152 (1964).

[14]R. K. Chang, J. Ducuing, N. Bloembergen, Phys. Rev. Letters 15, 6 (1965).

L545 4-4

Reprinted from
Volume 6, Number 10 APPLIED PHYSICS LETTERS May 15, 1965

APPENDIX 3

MULTIMODE EFFECTS IN THE GAIN OF RAMAN AMPLIFIERS AND OSCILLATORS[1] I. OSCILLATORS

P. Lallemand
Gordon McKay Laboratory, Harvard University
Cambridge, Massachusetts

N. Bloembergen[2]
Departments of Electrical Engineering and Physics
Berkeley, California

(Received 19 March 1965)

(Stokes pumping; ruby laser excitation; E/T)

Although a great deal of experimental work has been done in the field of stimulated Raman emission, quantitative measurements on the Raman gain have been sparse. The interpretation of such data[3-5] is complicated by the multimode structure of the laser beam.[6] In this Letter experimental evidence for these multimode effects is presented. It is found that the gain per unit length in a Raman cell may vary by a factor five or more. The behavior of Raman oscillators is also profoundly affected by the mode structure of the exciting laser beam. The unfocused beam of 2-mm diam used in our experiments has an "étendue", or number of spatial modes, equal to 25. This number is defined as the product of the area of

the beam with the solid angle it subtends, divided by the square of the wavelength. It is important to attenuate the laser beam without changing the mode structure. Since the laser beam is linearly polarized, this can be accomplished by the use of a Glan-Thompson prism. The beam passes through a Raman oscillator cell of variable length, as one window moved as a piston in the cylindrical cell. The windows were not coated and were not optically parallel. No provision was made to control the feedback. The emitted Stokes intensity was measured by a photocell with suitable filters, which accepted the relatively large solid angle of 6×10^{-3} steradian. The stimulated Stokes radiation is emitted in a solid angle of about 2×10^{-5} steradian. Second- and third-order Stokes intensities could also be measured with appropriate filters. Figure 1 shows the intensity of first and second Stokes light in nitrobenzene as a function of the length of the Raman cell at constant laser intensity $\mathcal{I}_L$. The curves as a function of laser intensity at constant length are essentially the same.

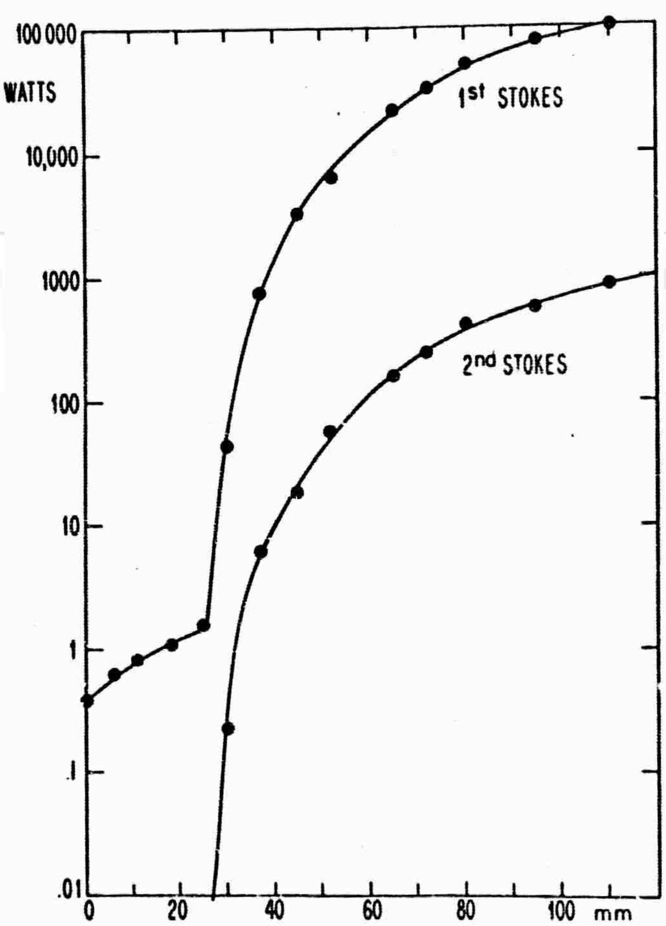

Fig. 1. Intensity of the first and second Stokes lines of nitrobenzene as a function of cell length, at constant laser intensity. The residual signal for $l = 0$ is due to the finite transmission of the filters at the ruby frequency. The curves of the Stokes intensity as a function of laser intensity at constant length l are essentially the same.

Similar curves have also been obtained for benzene and other fluids.

At very low intensity only spontaneous Raman emission is observed, which is initially proportional to $\mathcal{I}_L$. The sharp break indicates the onset of regenerative feedback. At this point the power gain in a single passage may be about 10^4 to 10^6 and diffuse reflection from the windows is sufficient to obtain regenerative oscillator action in one spatial mode. If only one mode is oscillating, the Stokes intensity should be given by a linear relationship, $\mathcal{I}_S = C(\mathcal{I}_L - \mathcal{I}_{\text{threshold}})$. This is not the case. Stokes radiation comes out in many modes at higher power levels, which utilize more and more modes or filaments of the incident laser beam. The total laser power is never significantly depleted. In the case of nitrobenzene a small depletion is observed which is, however, due to two-quanta absorption. Apparently a large fraction of the laser flux does not participate in Stokes pumping. The observed Stokes intensity is well represented by

$$\mathcal{I}_S = \sum_i C_i(\mathcal{I}_L - \mathcal{I}_{i,\ \text{threshold}})$$

There is a distribution of thresholds. Many modes have a threshold three or more times higher than the lowest. This is in agreement with the considerations of Bloembergen and Shen.[6]

The second Stokes intensity builds up in a similar manner as the Stokes intensity. This second Stokes is not generated parametrically by a polarization $P_{SS}(\omega_{SS}) = \chi^{NL} E_S^2 E_L^*$. In this case the second Stokes radiation should come out preferentially in a cone and its intensity $\mathcal{I}_{SS}$ should be proportional to $\mathcal{I}_S^2$. This is not observed. The second Stokes ring has an intensity of the order of 1% of the forward emission and can be photographed only when using a long cell. The second Stokes is created by a Raman process, in which $\mathcal{I}_S$ serves as pump. As soon as the threshold is exceeded in the first filament, its Stokes intensity builds up rapidly depleting the laser power in this filament.[7] It is soon capable of creating $\mathcal{I}_{SS}$ in the same filament, while other Stokes modes just above their threshold are not yet capable of doing so. As the gain in the Raman cell is increased, ever more Stokes modes are fired, which in turn excite an ever growing number of second Stokes modes, etc. This is the reason why the higher order Stokes intensities all appear to build up in a similar manner. This effect has also been observed by Bret,[8] and Takuma and Jennings.[5]

[1]This research is supported by Project Defender of the Office of Naval Research.
[2]On leave from Harvard University.

Reprinted from

Volume 6, Number 10 APPLIED PHYSICS LETTERS May 15, 1965

[3] R. W. Hellwarth, *Appl. Optics* **2**, 847 (1963).
[4] G. Bret, *Compt. rend.* **259**, 2991 (1964).
[5] H. Takuma and D. A. Jennings, *Proc. IEEE* **53**, 146 (1965).
[6] N. Bloembergen and Y. R. Shen, *Phys. Rev. Letters* **13**, 720 (1964).
[7] Y. R. Shen and N. Bloembergen, *Phys. Rev.* **137**, A 1787 (1965).
[8] G. Bret and G. Mayer, *Compt. rend.* **258**, 3265 (1964).

MULTIMODE EFFECTS IN THE GAIN OF RAMAN AMPLIFIERS AND OSCILLATORS[1] II. AMPLIFIERS

P. Lallemand
Gordon McKay Laboratory, Harvard University
Cambridge, Massachusetts
N. Bloembergen[2]
Departments of Electrical Engineering and Physics
Berkeley, California

(Received 19 March 1965)

(Stokes pumping; ruby laser excitation; E/T)

The high exponential gain and feedback in Raman oscillators[3] make a quantitative interpretation of experimental results obtained by their use quite difficult. When the Raman gain is measured instead with amplifier cells, this difficulty disappears and consequently more interesting conclusions can be drawn than was the case for oscillators. The laser and Stokes radiation created in a Raman oscillator traverse a variable distance d before entering an amplifier cell of variable length l. The laser intensity is adjusted so that no regenerative oscillation occurs in the second cell. The Stokes intensity is attenuated by suitable filters and is measured at the input by a beam splitter and at the output. The aperture is confined so that only Stokes radiation within the confines of the laser beam is accepted. The gain in the amplifier has been measured as a function of the length l as well as of the separation d. Figure 1 shows that the overall gain is a sensitive function of the separation d. Furthermore, the gain per unit length $\{d[ln(\mathcal{I}_s/\mathcal{I}_0)]\}/dx$ in the cell is considerably smaller in the first few centimeters than at larger distances from the cell front.

Both remarkable facts are readily explained by the multimode theory. If the separation d between the cells is sufficiently long, the intensity pattern of the Stokes radiation at the input of the second cell will not have an optimum correspondence with the intensity pattern at the laser frequency. A decomposition of the Stokes input into new normal modes corresponding to the laser intensity distribution in the amplifier cell is necessary. Many modes will grow with the average gain, which is represented by the initial slope of the gain curve. Eventually the mode with highest gain will take over. This gain is represented by the steep part of the curves. Since the insertion loss for the mode with maximum gain is

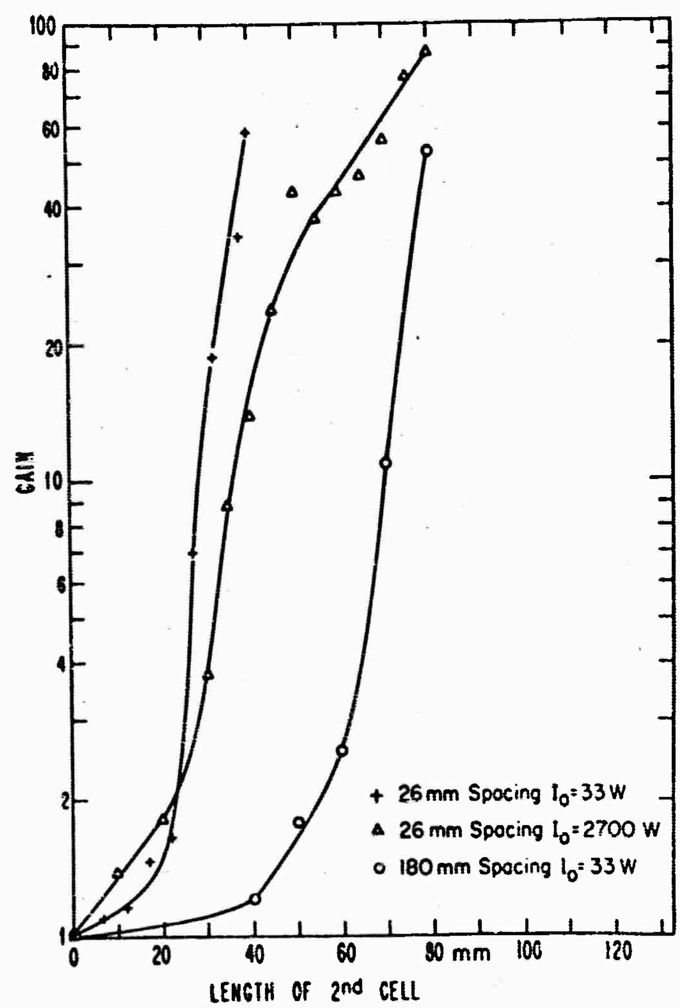

Fig. 1. Stokes gain in a second Raman cell in series with a Raman oscillator cell as a function of amplifier cell length l for different values of the spacing d between the two cells and of the input Stokes intensity $\mathcal{I}_0$.

larger for larger separations d, it takes longer for this mode to emerge for large d. Ordinarily the gain per unit length is taken to be proportional to the Raman susceptibility and the average laser intensity. This gain corresponds more nearly to the initial slope rather than the maximum slope in the amplifier cell. Large systematic errors may therefore have occurred in previous determinations of the Raman susceptibility. The effect of saturation due to the depletion of the laser power in the mode with maximum gain is evident in the curve of Fig. 1 for the larger Stokes input power. This saturation mechanism is, of course, responsible for limiting the Stokes power in a Raman oscillator. These effects may be caused both by the spatial and the temporal intensity structure of the laser beam.

The spatial multimode effect can be demonstrated[4] in a striking manner by splitting a laser beam into beams of equal intensity which excite Stokes radiation in identical Raman cells, as shown in Fig. 2. If the beam splitter is of good optical quality, with a tolerance less than $\lambda/20$, the intensities of the two Raman cells in parallel have a very good one-to-one correspondence in each pulse. The relative rms deviation in the intensity ratio $\mathcal{S}_A/\mathcal{S}_B$ is about 0.2. When the beam splitter has a tolerance in flatness of $\lambda/2$, this rms deviation increases by a factor three to 0.6. In this case significant differences in the mode structure of the split beam in the two cells are present during each pulse.

The Raman amplifier cell will be very useful for a quantitative study of the gain as a function of the state of polarization of the Stokes and laser polarization. In principle all three constants[5] of the Raman susceptibility tensor in isotropic fluids may be measured. It may also be possible to measure the Raman gain at Stokes frequencies which are not emitted in Raman lasers, because the corresponding vibrations give too high a threshold. The amplifier cell will also be used by us to unravel further the relationships in mixtures of Raman fluids, which have recently been reported by Kaiser, Maier, and Giordmaine.[6] When a more powerful laser beam with a larger cross section becomes available, the angular dependence of the gain at Stokes and anti-Stokes frequencies[7] may also be studied more quantitatively with the amplifier cell.

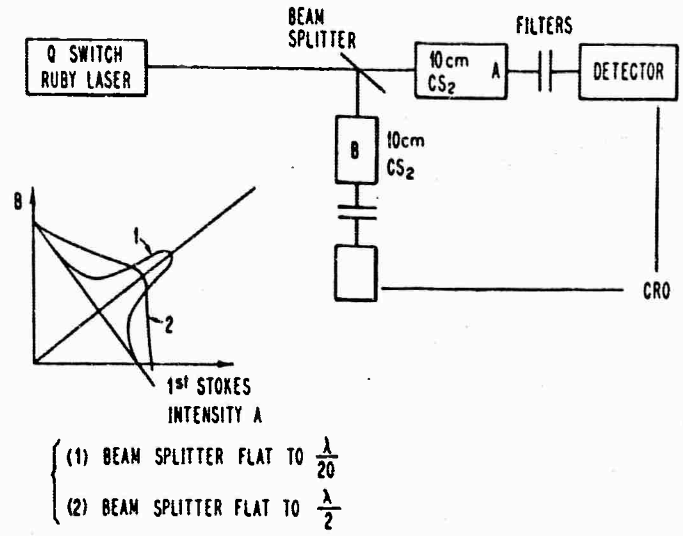

Fig. 2. Experimental set-up to show the influence of the spatial multimode structure of the laser light on Stokes production. The diagrammatic insert shows the scattering in the ratio of the Stokes intensities in cells *A* and *B* from each laser pulse.

[1]This research is supported by Project Defender of the Office of Naval Research.

[2]On leave from Harvard University.

[3]P. Lallemand and N. Bloembergen, preceding paper.

[4]J. Ducuing and N. Bloembergen, *Phys. Rev.* **133**, 1493 (1964).

[5]P. D. Maker and R. W. Terhune, *Phys. Rev.* **137**, A801 (1965).

[6]W. Kaiser, M. Maier, and J. A. Giordmaine, *Appl. Phys. Letters* **6**, 25 (1965).

[7]Y. R. Shen and N. Bloembergen, *Phys. Rev.* **137**, A1787 (1965).

APPENDIX 4

Light Waves with Exponential Gain*

N. Bloembergen
Department of Electrical Engineering, University of California, Berkeley, California

P. Lallemand
Gordon McKay Laboratory, Harvard University, Cambridge, Massachusetts

The coupled-wave formalism is reviewed to give a unified description of parametric down conversion of light, the stimulated Brillouin and Raman effects, stimulated light scattering in plasmas, etc. The exponential character of the gain is emphasized. The feedback in oscillators and the filamentary or multimode structure of the light beams present serious difficulties for quantitative measurements. Some experimental data on the gain in a Stokes amplifier cell are presented. The exponential gain constant for the benzene Stokes line has been measured as a function of polarization and of concentration in liquid mixtures. The relationship to the spontaneous-emission cross section in these cases is discussed.

THREE COUPLED LIGHT WAVES

The nonlinearity of an electromagnetic medium leads to a coupling between waves, which are the eigensolutions of the wave equation in the absence of the nonlinearity.[1] The coupling between three electromagnetic waves was considered in the theory of microwave parametric amplifiers, and the coupling between three and more light

*This research was supported by Project Defender of ARPA and the Office of Naval Research.

waves was treated early in the development of nonlinear optics.[1-3] The three nonlinear coupled equations in a piezoelectric crystal can be written in the form

$$\nabla^2 E_s + \frac{\epsilon_s \omega_s^2}{c^2} E_s = -\frac{4\pi\omega_s^2}{c^2} \chi^{NL} E_L E_i^* e^{i\Delta k \cdot r}$$

$$\nabla^2 E_i^* + \frac{\epsilon_i^* \omega_i^2}{c^2} E_i^* = -\frac{4\pi\omega_i^2}{c^2} \chi^{*NL} E_L^* E_s e^{i\Delta k \cdot r} \tag{1}$$

$$\nabla^2 E_L + \frac{\epsilon_L \omega_L^2}{c^2} E_L = -\frac{4\pi\omega_L^2}{c^2} \chi^{NL} E_i E_s e^{-i\Delta k \cdot r}$$

Often the laser amplitude E_L may be considered as a constant parameter, since the reaction on it by the much weaker fields at E_s and E_i is negligible. For $\Delta k = 0$ and idler damping large compared to the signal damping, one obtains a power gain at ω_s

$$g_s = -2\alpha_s + \left(\frac{4\pi\omega_i\omega_s^2}{c^2}\right)^2 \frac{|\chi^{NL}|^2 |E_L|^2}{k_L k_s \alpha_i} \tag{2}$$

If the exponential gain is sufficient to overcome coupling and diffraction losses, the system will become unstable and oscillations will start.

Giordmaine and Miller[4] have very recently succeeded in operating a tunable light oscillator based on this parametric down-conversion instability. The phase-matching condition in a $LiNbO_3$ crystal can be realized for three collinear light beams. The momentum matching depends sensitively on the temperature and allows thermal tuning of the parametric oscillator.

COUPLING BETWEEN TWO LIGHT WAVES AND ONE VIBRATIONAL WAVE

The stimulated Raman effect and the stimulated Brillouin effect can be described in the same manner.[1,5] One must replace the idler-wave equation in the coupled set by the wave equation for acoustical phonons in the case of the Brillouin effect and by the wave equations for optical phonons in the case of the stimulated Raman effect. The coupling constants are now proportional to the photoelastic constant and the electronic-vibrational coupling, respectively. It is also possible to replace the idler wave by a plasma wave or spin wave. This

coupling of light waves with plasmons and magnons is discussed elsewhere in these proceedings.

The set of coupled equations for the optical phonon wave Q_V and the Stokes wave E_S is

$$\beta\nabla^2 Q_V^* + (\omega_0^2 - \omega_V^2)\, Q_V^* + 2i\,\omega_V \Gamma_V Q_V^* = N(\partial\alpha/\partial Q) E_L^* E_S \tag{3}$$

$$\nabla^2 E_S + (\epsilon_S \omega_S^2/c^2) E_S = -4\pi(\omega_S^2/c^2) N(\partial\alpha/\partial Q) Q_V^* E_L \tag{4}$$

with $Q_V = R(2\rho)^{1/2}$, where R is the internuclear distance and $\rho = N\mu_V$ is the reduced mass density of the vibration for N molecules per unit volume, each with a reduced vibrational mass μ_V. The group velocity $d\omega/dk_V$ of the optical phonons is very small. The frequency of the optical phonon is essentially independent of the direction of the Stokes wave, $\omega_V = \omega_0 - \beta(k_L - k_S)^2/\omega_0 \approx \omega_0$. For forward Stokes scattering the phase velocity of the optical phonon is equal to the phase velocity of the light waves. For backward scattering the phase velocity is about twenty times slower for typical vibrational frequencies. The steady-state gain is now always reached during the giant laser pulse. Because of the low group velocity and the relatively strong vibrational damping, the exponential Stokes power gain per unit length may be written

$$g_S = \frac{8\pi^2\epsilon_S}{\lambda_S}\,\frac{N^2(\partial\alpha/\partial Q)^2}{2\omega_V\Gamma_V}\,|E_L|^2 = \frac{8\pi^2\epsilon_S(-\chi_S'')}{\lambda_S}\,|E_L|^2 \tag{5}$$

Here λ_S is the Stokes wavelength in the medium. The Stokes Raman susceptibility has been introduced by

$$-\chi_S'' = \frac{N^2(\partial\alpha/\partial Q)^2}{2\omega_V\Gamma_V} = \frac{N(\partial\alpha/\partial R)^2}{2\mu_V\omega_V\Gamma_V} \tag{6}$$

COUPLING WITH ANTI-STOKES WAVES

The vibrational wave and the laser wave also couple to the anti-Stokes wave at $\omega_a = \omega_L + \omega_V$. If initially only the laser amplitude is different from zero, the anti-Stokes waves cannot be generated. This case of parametric up-conversion has also been discussed extensively for three light waves. When the vibrational mode is heavily damped and the solution analogous to the Stokes wave is written down, one finds that the sign of g_S, or equivalently the sign of the imaginary part of the nonlinear susceptibility, has changed.

There is exponential loss at the anti-Stokes frequency, which has been called stimulated absorption by Stoicheff and coworkers.[6]

When the momentum-matching conditions for Stokes and anti-Stokes waves are simultaneously satisfied, $\mathbf{k}_V = \mathbf{k}_L - \mathbf{k}_S = \mathbf{k}_a - \mathbf{k}_L$, a set of four coupled waves at ω_L, ω_V, ω_S, and ω_a must be solved simultaneously. If the laser field is again treated as a constant parameter and the vibrational wave is eliminated because of heavy damping and low group velocity, one retains a set of two linearized coupled equations for E_S and E_a^*.

$$\begin{aligned} \nabla^2 E_S + \epsilon_S(\omega_S^2/c^2)E_S &= 4\pi(\omega_S^2/c^2)[\chi_S|E_L|^2 E_S + (\chi_a^* \chi_S)^{1/2} E_L^2 E_a^*] \\ \nabla^2 E_a^* (\omega_\alpha^2/c^2) E_a^* &= 4\pi(\omega_a^2/c^2)[(\chi_a^* \chi_S)^{1/2} E_L^{*2} E_S + \chi_a^* |E_L|^2] E_a^* \end{aligned} \tag{7}$$

There is one mode with exponential gain which has an appreciable anti-Stokes character near the phase-matched direction. This exponential gain at ω_a explains the copious production of anti-Stokes rings. The formal solution gives zero exponential gain for exact matching $\mathbf{k}_S + \mathbf{k}_a = 2\mathbf{k}_L$ of the unperturbed propagation vectors in the medium.[7] In this case each of the two coupled eigenmodes has 50 per cent Stokes and anti-Stokes character. This point has been discussed by several authors.[8] It is a rather academic point, however, because the dip to zero has an extremely narrow angular width $\Delta\theta \approx \Delta k/k \approx g_S\lambda$. Since the gain g_S rarely exceeds unity, i.e., an e-folding length of 1 cm, one has $\Delta\theta < 10^{-4}$ rad. A finite cross section of the beam, if it is confined to less than 1 cm in diameter as is always the case experimentally, or a nonuniform intensity distribution across the beam as would be the case if gain in lateral directions is allowed,[8] will obliterate this sharp dip in the gain. There is exponential gain at the anti-Stokes frequency near the phase-matched direction, and as a result the Stokes character of the wave is not 100 per cent. There is a drop in the Stokes intensity near the phase-matched direction, as has been observed by Chiao and Stoicheff[9] and by Garmire.[10]

The Stokes and anti-Stokes waves can acquire such intensities that they noticeably deplete the laser beam and can in turn create higher-order waves. The set of coupled wave equations then becomes very complex.

MULTIMODE EFFECTS

This complexity is compounded by the fact that the incident laser beam usually cannot be represented by a single homogeneous mono-

chromatic plane wave. The Stokes and anti-Stokes radiation of various orders is observed to have a distribution of directions and frequencies that implies the participation of a very large number of modes.[11] As in all instability problems, the modes with the maximum gain have to be found.

In practice the laser and Stokes intensity patterns cannot be described simply as the interference pattern of two or more plane waves. As will be discussed in more detail in the concluding section, after presentation of experimental data, one may expect patterns of hot filaments, changing with time during the pulse. Because of the nonlinear nature of the phenomena, the observed gain for a given total laser output can be an order of magnitude larger than the gain calculated for a uniform field.

POLARIZATION MODES. RELATION BETWEEN THE RAMAN TENSOR AND SPONTANEOUS EMISSION

Even if the direction and the frequency of the laser and Stokes waves are completely defined, there remains the twofold degeneracy of the polarization. One therefore has strictly speaking always to solve at least the two coupled equations for the two Stokes polarizations. Consider, for simplicity, the case of a Raman liquid. In an isotropic medium the Stokes polarization is completely specified by three components of the Raman susceptibility tensor,[12]

$$P(\omega_S) = \chi_1^{\text{Raman}} \mathbf{E}_S(\mathbf{E}_L \cdot \mathbf{E}_L^*) + \chi_2^{\text{Raman}} \mathbf{E}_L(\mathbf{E}_S \cdot \mathbf{E}_L^*) + \chi_3^{\text{Raman}} \mathbf{E}_L^*(\mathbf{E}_L \cdot \mathbf{E}_S)$$

It should be borne in mind that the Raman susceptibility is a complex quantity which obeys the same Kramers-Kronig relation as a linear susceptibility. Exactly at resonance it is pure imaginary. The real part is often equally important, since the observed frequency distribution of higher-order Stokes and anti-Stokes radiation shows that one often works in the wings of the vibrational resonance. All equations retain their validity for complex χ.

Consider the case that both the laser and the Stokes wave propagate in the z direction. The amplitudes E_{xL} and E_{yL} are treated as fixed parameters. The set of coupled equations for the two Stokes polarizations is

$$\nabla^2 E_{xs} + \epsilon_s(\omega_s^2/c^2)E_{xs} =$$
$$-(4\pi\omega_s^2/c^2)[(\chi_1 + \chi_2 + \chi_3)|E_{xL}|^2 + \chi_1|E_{yL}|^2]E_{xs}$$
$$+ (4\pi\omega_s^2/c^2)(\chi_2 E_{xL}E_{yL}^* + \chi_3 E_{xL}^* E_{yL})E_{ys}$$

$$\nabla^2 E_{ys} + \epsilon_s(\omega_s^2/c^2)E_{ys} =$$
$$-(4\pi\omega_s^2/c^2)(\chi_2 E_{xL}^* E_{yL} + \chi_3 E_{yL}^* E_{xL})E_{xs}$$
$$+ (4\pi\omega_s^2/c^2)[\chi_1|E_{xL}|^2 + (\chi_1 + \chi_2 + \chi_3)|E_{yL}^2|]E_{ys}$$

The eigenmodes may be solved for the case of general elliptical polarization of the incident laser beam. Two particular cases are evidently of special interest.

1. **The laser beam is linearly polarized.**

In this case we may put, without loss of generality, $E_{yL} = E_{yL}^* = 0$. The Stokes beam E_{sx} polarized parallel to the laser beam has a power gain

$$g_{s,\parallel} = -(8\pi^2\epsilon_s/\lambda_s)(\chi_1'' + \chi_2'' + \chi_3'')|E_{xL}|^2 \tag{8}$$

This is the Stokes radiation that has been observed in Raman oscillators. The perpendicular eigenmode E_{ys} has a gain

$$g_{s,\perp} = -(8\pi^2\epsilon_s/\lambda_s)\chi_1''|E_{xL}|^2 \tag{9}$$

In a Raman oscillator only the linear mode with the larger gain will be excited. The corresponding real parts represent a birefringence of the liquid, induced by the laser beam. Terhune[13] has observed an intensity-dependent index of refraction on the laser beam itself. The effect should, however, be particularly large on a Stokes line just off the vibrational resonance, where the real part is enhanced.

2. **The laser beam is circularly polarized.**

In this case we may take E_{xL} real and write $E_{xL} = iE_{yL} = E_{0L}$. Solution of the coupled wave equations shows that the Stokes eigenmodes are now also circularly polarized. The Stokes mode with the same sense of polarization as the laser beam has a power gain

$$g_{s,\mathrm{same}} = -(8\pi^2\epsilon_s/\lambda_s)\,E_{0L}^2(\chi_1'' + \chi_2'') \tag{10}$$

while the mode with the opposite sense of polarization has the gain constant

$$g_{s,\mathrm{opposite}} = -(8\pi^2\epsilon_s/\lambda_s)\,E_{0L}^2(\chi_1'' + \chi_3'') \tag{11}$$

The output of a Raman oscillator, pumped with a circularly polarized laser beam, will itself be circularly polarized. Similar considerations hold for the stimulated Brillouin effect in liquids.

The real parts of these susceptibilities now lead to the phenomenon of light-induced optical activity. In the presence of circular polarized laser light, the plane of polarization of a linear polarized beam at another frequency will turn. This effect should again be pronounced for Stokes light just off the vibrational resonance, where the real parts of these susceptibilities will have the largest difference. In principle the three components can be determined by measuring the gain constants in these geometries.

It has been shown in Eq. (6) that the Raman susceptibility is proportional to the derivative of the electronic polarizability of a molecule with respect to internuclear distance $\partial\alpha/\partial Q$. In the same manner, the tensorial or anisotropic properties of this susceptibility are related to the anisotropic properties of the polarization derivatives of a molecule, suitably averaged over all molecular orientations in the liquid.[14] This procedure was developed by Placzek[15] and has been reviewed in books on spontaneous Raman scattering.[16]

Consider an anisotropic molecule with principal polarizabilities α_1, α_2, and α_3. Define a scalar part a and an anisotropic part b by

$$a = \frac{1}{3}(\alpha_1 + \alpha_2 + \alpha_3)$$

$$b = \left[\frac{1}{2}(\alpha_1 - \alpha_2)^2 + \frac{1}{2}(\alpha_2 - \alpha_3)^2 + \frac{1}{2}(\alpha_3 - \alpha_1)^2\right]^{1/2}$$

Take the derivatives of these quantities with respect to the normal coordinate Q of the totally symmetric vibration of the molecule

$$a = a_0 + (\partial a/\partial Q)Q = a_0 + a'Q$$

$$b = b_0 + (\partial b/\partial Q)Q = b_0 + b'Q$$

Calculate the square of $(\partial\alpha/\partial Q)$ for the particular Raman polarization of interest for a given molecular orientation, and average over all orientations in the isotropic liquid. In this manner one finds that the Raman gain for the modes with a linear polarized laser beam is proportional to

$$\begin{aligned} \chi_1'' + \chi_2'' + \chi_3'' &= -N(45a'^2 + 4b'^2)/2\mu_v\omega_v\Gamma_v \\ \chi_1'' &= -3Nb'^2/2\mu_v\omega_v\Gamma_v \end{aligned} \qquad (12)$$

For the circular polarized modes the gain is proportional to

$$\chi_1'' + \chi_2'' = -N(45a'^2 + b'^2)/2\mu_V\omega_V\Gamma_V$$
$$\chi_1'' + \chi_3'' = -6Nb'^2/2\mu_V\omega_V\Gamma_V \tag{13}$$

The three components of the Raman susceptibility tensor can therefore be expressed in terms of two independent quantities a′ and b′. This is true if ω_L and ω_S are sufficiently far removed from electronic resonances so that the antisymmetric part of the susceptibility tensor can be ignored.[15] The relation of a′ and b′ to the symmetry properties of a molecule is well known. For totally symmetric vibrations a′ and b′ can assume arbitrary values, except for symmetric molecules such as CCl_4 belonging to a cubic class; in this case b′ = 0. For antisymmetric vibrations a′ must vanish.

Note that the ratios of the stimulated Raman gain factors are the same as the depolarization and inversion factors for spontaneous Raman emission in the corresponding geometries. This remains true if interactions between molecules and local field corrections in the liquid are taken into account. Precisely the same correction factors apply in both cases. The polarization tensor $\boldsymbol{\alpha}$ must be replaced by $L(\omega_L) \cdot \boldsymbol{\alpha} \cdot L(\omega_S)$ where $L(\omega)$ is the Lorentz local field tensor. For a liquid without associative effects of the neighboring molecules the Lorentz correction factor on the Stokes intensity is the scalar quantity $[\epsilon(\omega_S) + 2]^2[\epsilon(\omega_L) + 2]^2/81$. This factor also applies to the spontaneous Raman emission. The acting laser field is now the field inside a Lorentz cavity. For the spontaneous emission at ω_S the mode wave function of the vacuum should be replaced by the mode wave function for the dielectric with the cavity. There is consequently a similar correction factor at ω_S. The ratio between stimulated emission and spontaneous emission remains $n_{ph}(\omega_S)$, where this excitation number of the field oscillator is proportional to the classical field intensity. The relationship between the total Raman scattering cross section for one particular mode of Stokes polarization, which radiates in a $\cos^2\theta$ pattern into the total solid angle 4π, and the Raman susceptibility for that same mode of polarization is

$$\chi_S'' = \frac{c^4}{\Gamma_V \hbar\omega_L \omega_S^3 \epsilon_S} \frac{3}{4\pi} \sigma_R \tag{14}$$

THE OUTPUT INTENSITY OF RAMAN OSCILLATORS

The Stokes ($\omega_S = \omega_L - \omega_V$) and second Stokes ($\omega_{SS} = \omega_L - 2\omega_V$) intensities of a Raman oscillator cell as a function of laser power are shown in Fig. 1. This particular example is for a 10-cm-long nitrobenzene cell. The output as a function of cell length at constant laser power shows a nearly identical behavior and has been published elsewhere.[17] This output behavior is representative of instabilities produced by laser beams. Similar curves have been obtained by Bret,[18] while Brewer[19] has observed the same trends for the Brillouin-shifted lines.

Although the windows in the particular cells with which Fig. 1 was obtained were not parallel, the onset of regenerative feedback is evident by the sharp break in the curve. At lower power levels spontaneous emission is observed. The feedback is perhaps caused

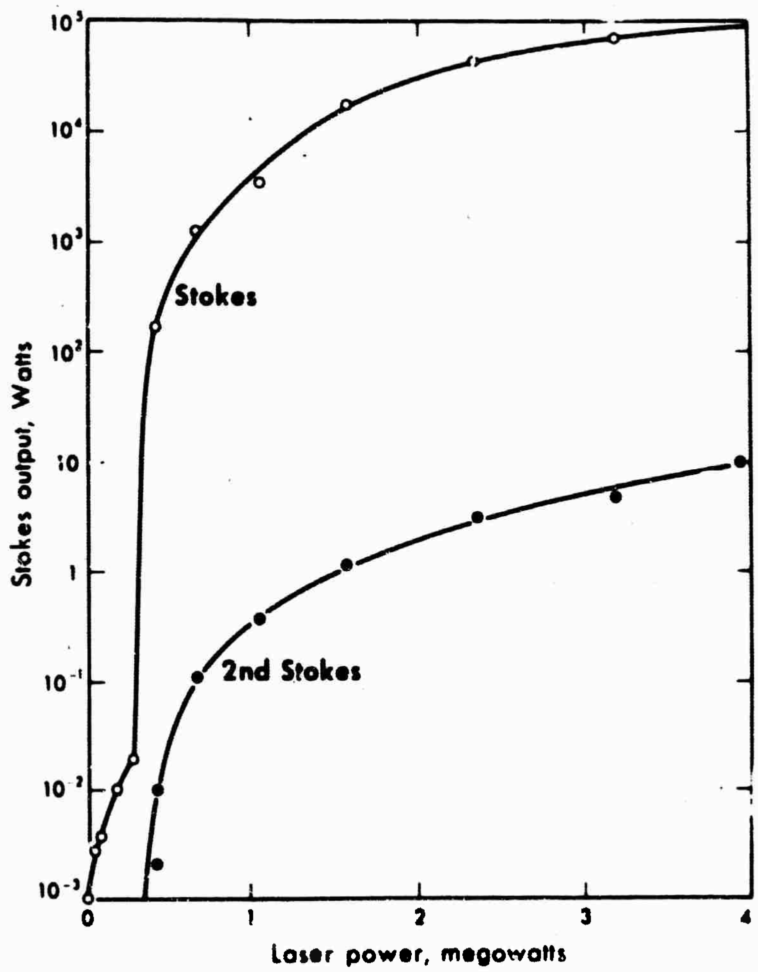

Fig. 1. The Stokes and second Stokes output intensity of a 10-cm-long nitrobenzene Raman cell, as a function of laser pump power.

by random-scattering centers, or it may be caused by a transverse instability of the laser beam discussed in the concluding section.

The following features show that the theory of pumping by a single uniform laser mode is inadequate.

1. Second (and higher) order Stokes radiation appears at almost the same threshold as the fundamental Stokes light.

2. Above threshold the output of a feedback oscillator should be a linear function of pump power. If the curve of Fig. 1 is plotted on a linear scale, it has a positive curvature.

3. For Raman cells longer than about 20 cm, the threshold becomes essentially independent of the reflectivity and parallelism of the windows. For very short cells, however, the feedback by reflection is important.

4. The laser power often does not get significantly depleted. The Stokes power in long cells usually does not exceed 1 per cent of the laser power in unfocused beams.

5. The Stokes generation is not a uniquely defined process but has some stochastic properties.

This last point is proved experimentally by splitting the laser beam and pumping two identical Raman cells in parallel.[17] There is no strict one-to-one correspondence between the outputs of the two cells. Since the rms deviations become larger when the beam splitter is of poor optical quality, this suggests a filamentary of multimode structure of the laser beam which varies from pulse to pulse. Stochastic variations in the laser-beam intensity may occur both in time and in space.

The Stokes output shown in Fig. 1 can be represented rather well by a linear combination of filaments with a distribution of laser powers ranging over an order of magnitude,

$$I_S = \Sigma C_j(I_{L,j} - I_{\text{threshold}})$$

This distribution may also explain the behavior of the second Stokes intensity. In the filaments with the highest laser intensity, the Stokes intensity builds up rapidly to pass the threshold for second Stokes generation, while in other regions the nonuniform Stokes intensity is not capable of doing so. Only a fraction of the total laser power is active in the stimulated Raman process because the exponential gain in regions of lower laser intensity is not sufficient. A quantitative determination of Raman gain and susceptibilities becomes very difficult under these circumstances.

The difficulties are enhanced if one takes into account the angular and frequency distribution of the Stokes radiation. The best meas-

urements would be made from the threshold in very short cells with a well-controlled feedback by reflecting mirrors. In this case one would obtain a measure of the gain in the "hottest" filament. The output of oscillators is of course always determined by some nonlinearity. The depletion of the laser intensity is the most likely limiting factor in Raman oscillators. For quantitative measurements and an experimental check of the exponential gain, stable amplifier cells must be preferred.

EXPONENTIAL GAIN IN RAMAN AMPLIFIER CELLS

It is, of course, possible to prevent the instability from developing by choosing the cell length sufficiently small and/or the laser pump intensity sufficiently low. In this case one has a stable amplifier with zero output for zero Stokes input, except for very weak spontaneous-emission noise. The experimental arrangement to measure the gain of the stable amplifier is shown in Fig. 2. Laser

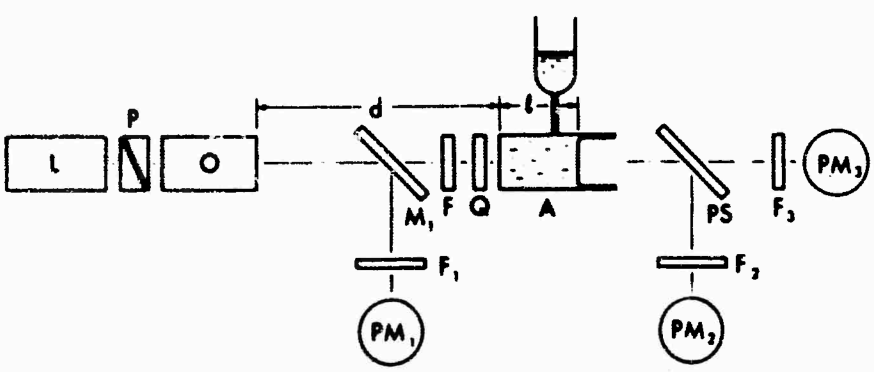

Fig. 2. Diagram of experimental arrangement for the gain measurement in a Raman amplifier cell.
L = ruby laser
P = Glan Thomson polarizer
O = Raman oscillator cell
M_1 = selective mirror, with a transmission loss of 30 db at ω_S and 1 db at ω_L
F, F_1, F_2, and F_3 = selective filters at ω_L and ω_S
Q = quartz retardation plate for selection of polarization at ω_L and ω_S
A = Raman amplifier cell of variable length 1
PS = polarization separator
PM_1 = photomultiplier monitor of Stokes input
PM_2 and PM_3 = photomultipliers monitoring the two polarizations of Stokes output

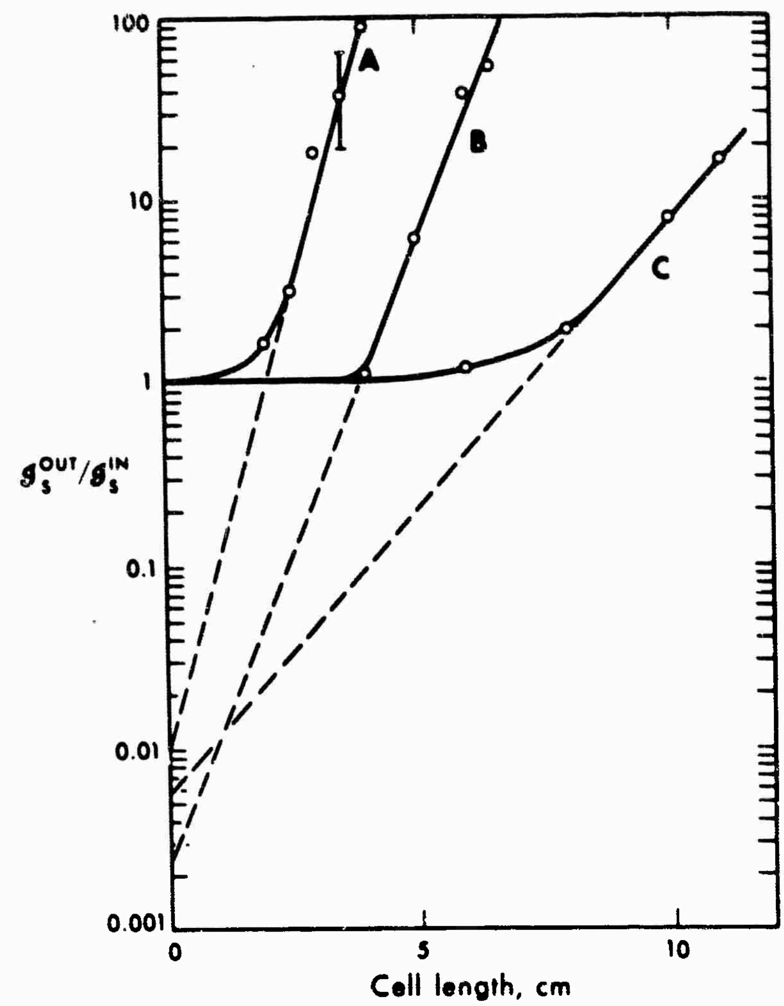

Fig. 3. The Stokes output to input ratio or gain of a benzene Raman amplifier cell as a function of cell length for three different laser pump power levels. The ratio of the laser intensities for curves A, B, and C is as 1:0.57:0.36, respectively. The intercepts of the straight high-gain parts with the intensity axis give the insertion loss of the Stokes input into the filament with highest gain.

and Stokes radiation is generated in a Raman oscillator. A selective reflector attenuates the Stokes radiation by at least 30 db and the laser pulse by about 1 db. The 30-db padding at ω_s isolates the amplifier from the oscillator. Additional selective absorbers at ω_L and ω_s may be inserted. The input Stokes power is monitored by a photomultiplier with suitable selective filters. The output Stokes power after the light beams have traversed an amplifier cell of variable length is measured by another photomultiplier, which is again supplied with calibrated filters and attenuators to ensure operation at a suitable intensity level.

The variation of the amplifier gain, defined as I_s^{out}/I_s^{in}, is plotted in Fig. 3 as a function of cell length 1 for three different laser power levels. Curve A was obtained for full laser power. In curves B and

C the laser power was attenuated by selective filters to 57 and 36 per cent of its full value, respectively. It is possible to exclude saturation effects experimentally. The same ratio I_S^{out}/I_S^{in} is obtained if the input intensity is changed by an order of magnitude.

The semilogarithmic plot shows that there is a region of exponential gain with a gain constant per unit length proportional to the laser power, given by the slope of the experimental plot. The remarkable feature is, however, that the initial slope is much smaller. The gain constant in the first few centimeters of the amplifier is at least an order of magnitude smaller than farther on. Furthermore, the region of low gain becomes longer the farther the amplifier is removed from the oscillator. An amplifier cell of fixed length l appears to have an overall gain which is a function of the separation d from the oscillator. The parameter d is clearly not an intrinsic property of the amplifier.

A satisfactory explanation of this curious behavior can be given in terms of a filamentary structure of the beams. At the output of the Raman oscillator the filaments of Stokes and laser radiation coincide in space and time. Since the Stokes radiation has an aperture of about 10^{-2} rad, an order of magnitude larger than the laser beam aperture, this match between the filaments at ω_L and ω_S is at least partially lost after a distance d ~ 100a, where a ~ $10^{-2} - 10^{-1}$ cm is a reasonable dimension for the filament. Smaller diameters of the filament are precluded by the observed angular definition of Stokes radiation. The gain of the amplifier depends on the spatial distribution of the Stokes input with respect to the filamentary structure of laser. One has a typical insertion loss for the Stokes input into each filament. The low initial slope should correspond to an average gain, as calculated from Eq. (5), if one determines $|E_L|^2$ from the average laser flux density. For benzene the low initial amplifier gain for laser and Stokes light polarized parallel to each other was found to be $g_S \sim 0.025$ cm^{-1} for a laser flux density of 10^7 watts/cm^2. According to Eq. (5), this corresponds to a Raman susceptibility of about 1.2×10^{-12} esu, in good agreement with the value determined from Eq. (13) for a total Raman scattering cross section $\sigma_R = 5.6 \times 10^{-29}$ cm^2, as determined by Damen, Leite, and Porto,[20] and a vibrational width $\Gamma_V = 3.1$ cm^{-1}.

The gain in the high-intensity filaments can be higher by as much as a factor of 60. This enhanced gain becomes evident when the Stokes intensity in these channels has built up to a dominant level. The curves in Fig. 2 show that the insertion loss into the high-gain channel is about a factor of 10^{-2} for the geometry used. When the mode structure of the laser is cleaned up, the observed gain en-

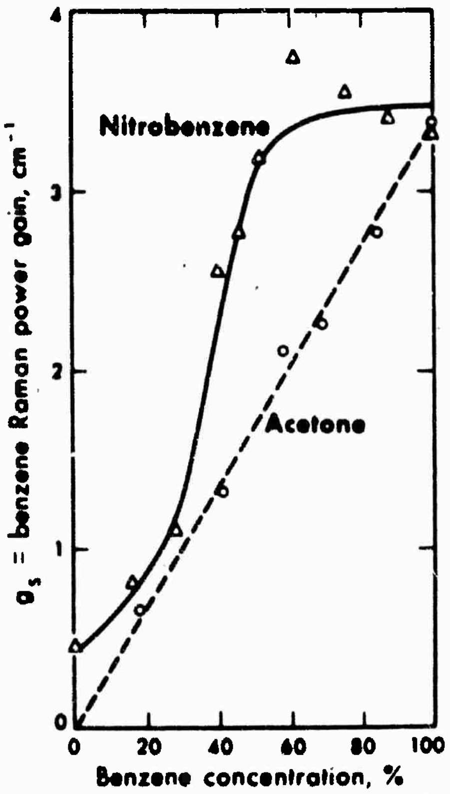

Fig. 4. The power gain constant per unit length g_S for the benzene Stokes line as a function of relative concentration in benzene-nitrobenzene (Δ) and benzene-acetone (o) mixtures.

hancement is reduced in agreement with the proposed model.

The linear parts of amplifier-response curves of the type shown in Fig. 3 may now be used to measure the Raman gain as a function of other variables. In Fig. 4 the gain per unit length of benzene Stokes radiation at 992 cm^{-1} is plotted as a function of the relative benzene concentration, when the amplifier cell is filled with benzene-acetone and benzene-nitrobenzene mixtures. For benzene-acetone the gain is a linear function of the relative benzene concentration. This behavior could be expected if there is little change in damping or local field due to interaction of the symmetric vibration with neighboring molecules. This linear dependence has also been observed for the spontaneous emission of the 992-cm^{-1} benzene line in mixed liquids.[21] This behavior should be contrasted with the Raman oscillator output of mixtures, where the interpretation is hazardous because of nonlinear competition between different oscillating modes.[22] The curve for the nitrobenzene-benzene mixture shows a remarkable behavior. The gain does not decrease down to 50 per cent benzene concentration. The decrease in the density of benzene molecules is apparently compensated by an increase in the Raman polarizability per molecule. This may be caused by stronger local field corrections or by a decrease in damping. The benzene Stokes

gain is not zero in pure nitrobenzene. This small gain can be explained by the presence of a nitrobenzene vibration at 1,000 cm^{-1}. It is clear that the Raman gain can in principle be measured for vibrations that normally do not show up in oscillators, because they do not have the opportunity to get above threshold.

Another example is the measurement of the Raman gain as a function of polarization. If one inserts before the amplifier a quartz plate of suitable thickness and orientation, so that it gives $1/4\lambda$ retardation at ω_L and $1/2\lambda$ retardation at ω_S, the Stokes gain for a linear input signal in the presence of a circular polarized pump can be measured. The input signal must be decomposed into two circular polarized components. Since these have different gain constants, g_{same} and g_{opp}, respectively, the output will become elliptically polarized. The polarization ellipse of the output can be analyzed in a well-known manner. The ratio of the major to minor axis is

$$\frac{\exp(g_{same}\,\ell) + \exp(g_{opp}\,\ell)}{\exp(g_{same}\,\ell) - \exp(g_{opp}\,\ell)}$$

The experimental results give for the ratio of the gain constants

$$\frac{g_{opp}}{g_{same}} = \frac{6b'^2}{45a'^2 + b'^2} = 0.44 \pm 0.05$$

A rotation of the axes of the ellipsoid would be a measure of the difference in the real parts of the Raman susceptibility for the two circular components. Although such an effect has been seen, our present data are not conclusive. The real part depends sensitively on the offset from exact vibrational resonance of the Stokes components.

When a quartz plate is used, which gives λ retardation at ω_S and $\lambda/2$ retardation at ω_L, the linear polarized Stokes input may be given an arbitrary angle with respect to the linear polarized laser beam by rotating the quartz plate. In this manner it was possible to measure the ratio of parallel to perpendicular gain

$$\frac{g_{\perp}}{g_{\parallel}} = \frac{3b'^2}{45a'^2 + 4b'^2} = 0.19 \pm 0.07$$

The inversion and anisotropy ratios are mutually consistent. They are, however, not compatible with the depolarization ratio determined from the angular dependence of spontaneous Raman scattering from a polarized beam of a gas laser. Daman, Leite, and Porto[20] give for benzene $6b'^2/(45a'^2 + 7b'^2) < 0.07$. The discussion above

under Polarization Modes shows unequivocally that the same constants a′ and b′ determine the polarization properties of both spontaneous and stimulated emission. The reason for this discrepancy is still obscure, but it will be discussed somewhat further in the concluding section.

DISCUSSION

The material properties of interest in the Raman effect, i.e., the components of the Raman susceptibility tensor, can be derived from Raman amplifier data. It is possible, in principle, to measure separately the effects of the real and imaginary parts. The imaginary part can be obtained, probably more simply and accurately, from the characteristics of spontaneous Raman scattering. The experiments of Terhune[23] on parametric generation of the anti-Stokes frequency away from the phase-matched direction give similar information about the absolute value of the Raman susceptibility.

The main interest of the Raman amplifier data, which are generally more useful for interpretation than oscillator data, lies perhaps in their information about the properties of the light beams. The high-intensity laser and Stokes beams cannot be considered as homogeneous distributions of constant intensity. Even if a laser initially emits a monochromatic diffraction-limited plane wave, such a uniform structure may not be preserved in the traversal of Brillouin or Raman media. Chiao, Garmire, and Townes[24] have pointed out the intensity-dependent focusing effect of light beams. These effects may be considerably enhanced if the real part of the Raman or Brillouin susceptibility near resonance is taken into account. Figure 3 shows that the Raman gain in a nominal 10 MW/cm^2 beam can be a factor e per centimeter, corresponding to an actual flux density in the filament of 400 MW/cm^2. If a Stokes component is 1 cm^{-1} removed from exact resonance to the side where $\chi_S' > 0$, the real part of the Stokes index of refraction, $2\pi\chi_S'|E_L|^2$, proportional to the intensity of the laser beam, may be as high as 10^{-4}. Since the laser intensity may vary appreciably over a lateral displacement a = 1 mm, gradients in the index of refraction for Stokes light as high as dn/dx $\approx 10^{-3}$ cm^{-1} would occur. The Stokes light from an area with radius a would be concentrated in a distance $\ell' \approx (na)^{1/2}(dn/dx)^{-1/2}$, or in a few centimeters, if a = 1 mm. This mechanism would favor the amplification of Stokes light, displaced somewhat to higher frequencies. As the Stokes intensity grows in the filament, its gradient in intensity will in turn focus the laser beam. It is not clear that a stable

steady situation with trapped beams will result. It seems more likely, in analogy to hydrodynamic instabilities, that a turbulent field is set up by this lateral instability. The possibility exists that the state of polarization of the light in this turbulent region is changed. This might account for the discrepancy between the anisotropy of stimulated Raman gain and the depolarization of spontaneous radiation.

Turbulent instability could also account for the stochastic nature of the gain measurements, for various other characteristics of the Raman amplifier discussed above, and for Raman gain anomalies when a single-mode laser beam is shone into a Raman cell as described by McClung.[25] Filamentary structure or multimode effects are, of course, other terms to describe inhomogeneities of the intensity in space and time. At the present time, the existence and importance of these nonuniform intensity distributions for stimulated gain processes seem to be well established, although their origin and detailed characteristics need further clarification.

REFERENCES

1. See, for example, N. Bloembergen, "Nonlinear Optics," W. A. Benjamin, Inc., New York, 1965.
2. R. H. Kingston, Proc. IRE, vol. 50, p. 472, 1962.
3. N. M. Kroll, Phys. Rev., vol. 127, p. 1207, 1962.
4. J. A. Giordmaine and R. C. Miller, Phys. Rev. Letters, vol. 14, p. 973, 1965.
5. Y. R. Shen and N. Bloembergen, Phys. Rev., vol. 137, p. 1787, 1965.
6. W. J. Jones and B. P. Stoicheff, Phys. Rev. Letters, vol. 13, p. 657, 1964.
7. See Figs. 4-13 and 4-14 in Ref. 1 or Figs. 1 and 9 in Ref. 5.
8. H. A. Haus, P. L. Kelley, and H. J. Zeiger, Phys. Rev., vol. 138, p. A960, 1965; C. L. Tang and T. F. Deutsch, Phys. Rev., vol. 138, p. A1, 1965.
9. R. Y. Chiao and B. P. Stoicheff, Phys. Rev. Letters, vol. 12, p. 290, 1964.
10. E. Garmire, this volume, p. 167.
11. N. Bloembergen and Y. R. Shen, Phys. Rev. Letters, vol. 13, p. 720, 1964.
12. P. D. Maker and R. W. Terhune, Phys. Rev., vol. 137, p. A801, 1965.

13. P. D. Maker, R. W. Terhune, and C. M. Savage, Phys. Rev. Letters, vol. 12, p. 507, 1964.
14. V. T. Platonenko and R. V. Khokhlov, Opt. Spectry. (USSR), vol. 18, p. 211, 1965.
15. G. Placzek, "Marx Handbuch der Radiologie," vol. 6, pt. II, pp. 209-374, Akademische Verlagsgesellschaft, Leipzig, 1934.
16. F. Kohlrausch, "Der Smekal-Raman Effekt," Ergänzungsband, Springer, Berlin, 1938.
17. P. Lallemand and N. Bloembergen, Appl. Phys. Letters, vol. 6, pp. 210, 212, 1965.
18. G. Bret, this volume, p. 180.
19. R. G. Brewer and D. C. Shapero, this volume, p. 216.
20. T. C. Damen, R. C. C. Leite, and S. P. S. Porto, Phys. Rev. Letters, vol. 14, p. 9, 1965.
21. See, for example, Ya. S. Bobovich, Soviet Phys. Usp., vol. 7, p. 656, 1965.
22. W. Kaiser, M. Mayer, and J. A. Giordmaine, Appl. Phys. Letters, vol. 6, p. 25, 1965.
23. See Ref. 12.
24. R. Y. Chiao, E. Garmire, and C. H. Townes, Phys. Rev. Letters, vol. 13, p. 479, 1964.
25. F. J. McClung, W. G. Wagner, and D. Weiner, this volume, p. 155.

APPENDIX 5

SELF-FOCUSING OF LASER BEAMS AND STIMULATED RAMAN GAIN IN LIQUIDS*

P. Lallemand† and N. Bloembergen

Gordon McKay Laboratory, Harvard University, Cambridge, Massachusetts
(Received 19 November 1965)

Anomalies in the gain of stimulated Raman processes in liquids have been investigated by several groups.[1-3] The study with a Stokes amplifier cell[4] revealed a regime where the gain per unit length was one to two orders of magnitude larger than the value calculated from the spontaneous Raman-emission cross section. The multimode theory of Bloembergen and Shen[5] is inadequate to explain this discrepancy, and the experiment of McClung[6] has shown that the same anomaly exists when the input laser power is essentially in a single mode. The amplifier cell studies[4] suggested that partially depolarized filaments of high intensity are formed as the laser beam passes through the liquid. This self-focusing action of laser beams was foreseen by Chiao, Garmire, and Townes,[7] Askarjan,[8] and Talanof.[8] It is due to the intensity-dependent index of refraction coupled with transverse gradients in the initial intensity distribution. This focusing action should be strongest in liquids with a large quadratic Kerr effect due to anisotropic polarizabilities of the molecules.[9] The purpose of this Letter is to describe new experimental results which support this view and extend the considerations of our very brief previous communication.[10] In the meantime Hauchecorne and Mayer[11] have independently arrived at similar conclusions on the basis of an elegant experiment. Shen and Shaham[12] have also carried out experiments with results similar to ours.

In a conventional Raman oscillator experiment with a collimated laser beam, one can define a threshold condition depending on pump

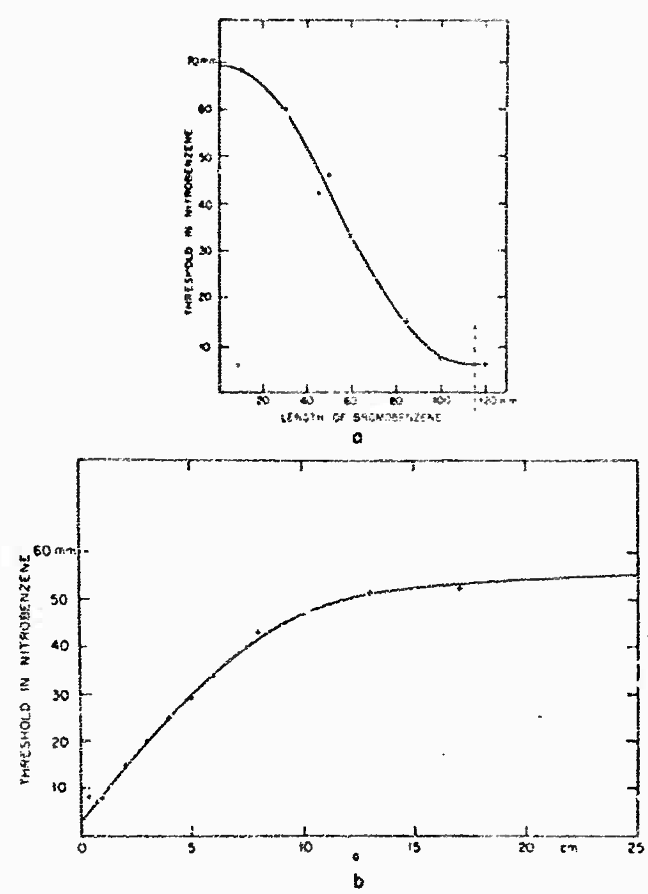

FIG. 1. (a) The threshold length for stimulated Stokes production in a nitrobenzene cell as a function of the length of a cell filled with bromobenzene placed immediately in front. The vertical dashed line indicates the threshold for Stokes production in bromobenzene. (b) The threshold length for stimulated Stokes production in a nitrobenzene cell preceded by a 30-cm long bromobenzene cell, as a function of the distance between the two cells.

intensity and cell length, such that $\mathscr{I}_{th} l_{th}^{x}$ = constant, where the exponent has the experimental range of value $1 < x < 2$. The threshold constant can be lowered significantly, if the laser beam first traverses a cell with another fluid. Figure 1(a) shows the reduction in the threshold length of a nitrobenzene cell as the length of a cell filled with bromobenzene and placed immediately in front of the nitrobenzene cell is increased. Note that the reduction occurs even before the first cell reaches its Stokes limit. The Stokes shift of the substance in the first cell is far from the nitrobenzene Stokes shift of 1345 cm^{-1}. In addition, filters are used to insure complete decoupling between the cells. The Stokes emission in the first cell may also be suppressed by selective absorbers without affecting the creation of hot filaments. The reduction of a factor 10 in threshold length means that the effective pump intensity is enhanced by almost two orders of magnitude. If the distance between the two cells is increased, the reduction is decreased. The effect of the first cell does not extend beyond 20 cm from its end face, as shown in Fig. 1(b). We have also shown the enhancement of intensity in filaments by means of another nonlinear process, the harmonic production in a quartz platelet placed at the end of the cell. This technique has been used in a more elegant and quantitative manner by Hauchecorne and Mayer.[11]

The creation of the filaments in the first cell has been recorded on a Polaroid film. The difficulty in making them visible for the cell lengths used in our experiments is that the main fraction of the laser intensity goes through without taking part in the focusing process. Since we had previous evidence that the effective pump light is partially depolarized, we put the cell between a crossed polarizer and analyzer to suppress most of the laser light. The image of the end face of the cell is recorded in Fig. 2. When the cell length is not sufficient for self-focusing, a weak homogeneous intensity distribution shown in Figs. 2(a) and 2(b) appears. When self-focusing occurs within the cell length, bright spots appear. Their number increases with increasing cell length. Their diameter is between 20 and 80 μ. This dimension is in agreement with the loss of the filamentary structure due to diffraction in 20 cm of air. The pattern changes from laser shot to laser shot, unless strong reproducible inhomogeneities are introduced into the beam by apertures. Figure 2(e) shows that filaments preferentially form in a circular pattern after diffraction of the beam through a circular hole before entering the cell.

There is a very good correlation between the self-focusing ability of a liquid and its intensity-dependent index of refraction.[9] Liquids are decreasingly effective in the order CS_2, nitrobenzene, bromobenzene, benzene, and acetone, while no detectable focusing action

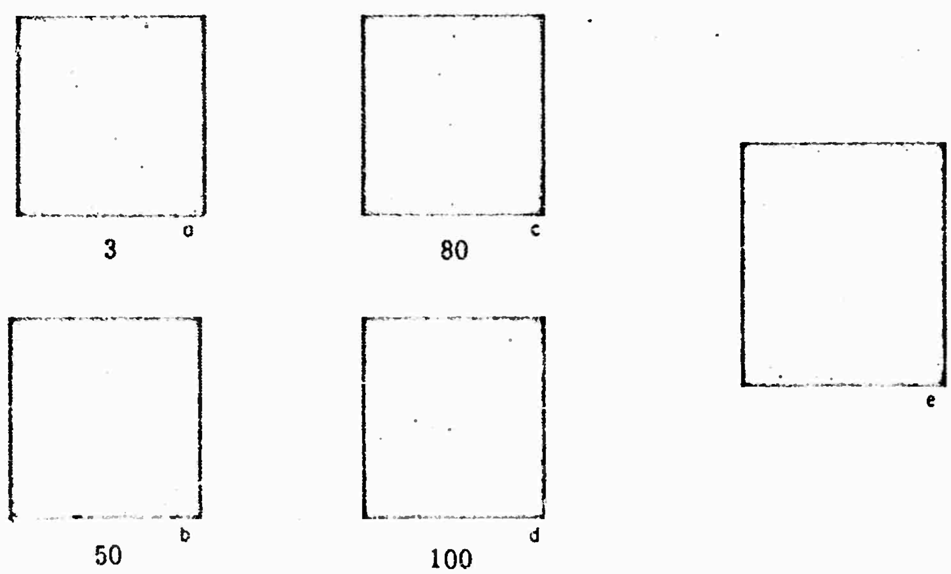

FIG. 2. Photographs of the end face of a nitrobenzene cell, between crossed polarizer and analyzer, of variable length indicated in mm. (a) and (b) The length is below threshold. (c) The length is at threshold for Stokes production. (d) The length is well above threshold. (e) The laser beam is diffracted by a small circular aperture before entering the cell. Filaments are found on rings of maximum transverse intensity gradient.

occurred with isopentane, alcohol, water, and CCl_4. We have found no good correlation with the electrostrictive properties nor with a resonance associated with two-quanta absorption. Theory also predicts that their contribution to the intensity-dependent index should be smaller than that of the anisotropic polarizability.

The experimental threshold for Raman laser action appears to be determined not so much by the value of the Raman susceptibility, but rather by the self-focusing capability of the fluid. This suggests that stimulated Raman oscillations may be induced in liquids that remain below threshold in the unfocused laser beam by mixing them with a focusing liquid. A cell with pure cyclohexane was below threshold in the collimated laser beam. Stimulated Stokes lines of cyclohexane were produced if the cell was filled with a mixture of two-thirds cyclohexane and one-third nitrobenzene. The totally symmetric CCl_4 molecule does not have sufficient focusing action of its own. We have observed three orders of stimulated Stokes light with the characteristic shift of 459 cm^{-1} of the totally symmetric vibration of CCl_4 in a mixture of 75 cc CCl_4, 15 cc nitrobenzene, and 10 cc CS_2. It was necessary to use a mixture of the last two focusing fluids in order to stay below the Stokes threshold of both of these.

The characteristic focusing length follows from the curvature of light rays in a transverse gradient of index of refraction. This length should be smaller than the Fresnel length of the beam, d^2/λ, and than the cell length. If the intensity drops by an amount $\mathcal{E}_0$ over a distance a on either side of an intensity maximum in the beam, the self-focusing length is

$$l_{\text{s.f.}} = \frac{a}{2}\left(\frac{n_0}{2n_2\mathcal{E}_0}\right)^{1/2},$$

where $n_2\mathcal{E}_0$ is the intensity-dependent change in index of refraction. A more detailed calculation of the focusing action in the laser beam has recently been given by Kelley.[13] If one takes a equal to the size of the laser beam d and puts $\mathcal{E}_0$ equal to the intensity at the beam center, he finds that the focusing length under the conditions of our experiments is 1 m for CS_2 with $n_2 = 10^{-11}$ esu; and 3 m for benzene with $n_2 = 0.2\times10^{-11}$ esu The experimental focusing lengths are an order of magnitude smaller. Furthermore, the whole beam does not focus as a unit. The multimode effect must still be invoked to explain this discrepancy. Apparently random small-scale intensity variations present in the input laser signal are responsible for more rapid and piecemeal focusing of the beam. It is not clear at this moment what factors determine the diameter of the filaments. Apparently some opposing defocusing effects set in after the filaments have reached a given size or intensity.

---

*This research is supported by the Office of Naval Research and the Advanced Research Project Agency.

†North Atlantic Treaty Organization, Office of Economic Cooperation, Europe, Fellow.

[1]G. Bret and G. Mayer, Compt. Rend. 258, 3265 (1964).

[2]P. Lallemand and N. Bloembergen, Appl. Phys. Letters 6, 210, 212 (1965).

[3]D. Weiner, S. E. Schwarz, and F. J. McClung, Appl. Phys. 36, 2395 (1965).

[4]N. Bloembergen and P. Lallemand in Proceedings of the International Conference on the Physics of Quantum Electronics, Puerto Rico, 1965, edited by P. L. Kelley, B. Lax, and P. E. Tannenwald (McGraw-Hill Book Company, Inc., New York, 1965).

[5]N. Bloembergen and Y. R. Shen, Phys. Rev. Letters 13, 720, (1964).

[6]F. J. McClung, W. C. Wagner, and D. Weiner, Phys. Rev. Letters 15, 96 (1965).

[7]R. Y. Chiao, E. Garmire, and C. H. Townes, Phys. Rev. Letters 13, 479 (1964).

[8]G. A. Askarjan, Zh. Eksperim i Teor. Fiz. 42, 1672 (1962) [translation: Soviet Phys.–JETP 15, 1161 (1962)]. W. I. Talanof, Izv. Vysshikh Uchebn. Zavedenii, Radiofizika 7, No. 3 (1964).

[9]F. Gires and G. Mayer, Compt. Rend. 258, 2039 (1964).

[10]N. Bloembergen and P. Lallemand, Bull. Am. Phys. Soc. 10, 1129 (1965).

[11]G. Hauchecorne and G. Mayer, to be published.

[12]Y. R. Shen and Y. Shaham, this issue [Phys. Rev. Letters 15, 1008 (1965)].

[13]P. L. Kelley, this issue [Phys. Rev. Letters 15, 1005 (1965)].

Unclassified
Security Classification

DOCUMENT CONTROL DATA - R&D

(Security classification of title, body of abstract and indexing annotation must be entered when the overall report is classified)

1. ORIGINATING ACTIVITY (Corporate author)
Office of Naval Research
Project Defender

2a. REPORT SECURITY CLASSIFICATION
Unclassified

2b. GROUP

3. REPORT TITLE
PROJECT DEFENDER

4. DESCRIPTIVE NOTES (Type of report and inclusive dates)
Final Technical Report

5. AUTHOR(S) (Last name, first name, initial)
Bloembergen, Nicolaas

6. REPORT DATE
February, 1966

7a. TOTAL NO. OF PAGES
48

7b. NO. OF REFS

8a. CONTRACT OR GRANT NO.
Nonr 1866

b. PROJECT NO.
NR-015-807

c.
49

d.

9a. ORIGINATOR'S REPORT NUMBER(S)
ARPA Order No. 455

9b. OTHER REPORT NO(S) (Any other numbers that may be assigned this report)
--

10. AVAILABILITY/LIMITATION NOTICES

11. SUPPLEMENTARY NOTES
--

12. SPONSORING MILITARY ACTIVITY
ONR - Project Defender

13. ABSTRACT

Experimental work on the second harmonic production of light in reflection from semiconductors and on the stimulated Raman effect in liquids is reviewed. Five published articles, partially supported under this contract, are reproduced as appendices.

DD FORM 1 JAN 64 1473

Unclassified
Security Classification

Unclassified

Security Classification

14. KEY WORDS	LINK A ROLE	LINK A WT	LINK B ROLE	LINK B WT	LINK C ROLE	LINK C WT
Nonlinear Optics						
Second Harmonic Light						
Stimulated Raman Effect						

INSTRUCTIONS

1. ORIGINATING ACTIVITY: Enter the name and address of the contractor, subcontractor, grantee, Department of Defense activity or other organization (*corporate author*) issuing the report.

2a. REPORT SECURITY CLASSIFICATION: Enter the overall security classification of the report. Indicate whether "Restricted Data" is included. Marking is to be in accordance with appropriate security regulations.

2b. GROUP: Automatic downgrading is specified in DoD Directive 5200.10 and Armed Forces Industrial Manual. Enter the group number. Also, when applicable, show that optional markings have been used for Group 3 and Group 4 as authorized.

3. REPORT TITLE: Enter the complete report title in all capital letters. Titles in all cases should be unclassified. If a meaningful title cannot be selected without classification, show title classification in all capitals in parenthesis immediately following the title.

4. DESCRIPTIVE NOTES: If appropriate, enter the type of report, e.g., interim, progress, summary, annual, or final. Give the inclusive dates when a specific reporting period is covered.

5. AUTHOR(S): Enter the name(s) of author(s) as shown on or in the report. Enter last name, first name, middle initial. If military, show rank and branch of service. The name of the principal author is an absolute minimum requirement.

6. REPORT DATE: Enter the date of the report as day, month, year; or month, year. If more than one date appears on the report, use date of publication.

7a. TOTAL NUMBER OF PAGES: The total page count should follow normal pagination procedures, i.e., enter the number of pages containing information.

7b. NUMBER OF REFERENCES: Enter the total number of references cited in the report.

8a. CONTRACT OR GRANT NUMBER: If appropriate, enter the applicable number of the contract or grant under which the report was written.

8b, 8c, & 8d. PROJECT NUMBER: Enter the appropriate military department identification, such as project number, subproject number, system numbers, task number, etc.

9a. ORIGINATOR'S REPORT NUMBER(S): Enter the official report number by which the document will be identified and controlled by the originating activity. This number must be unique to this report.

9b. OTHER REPORT NUMBER(S): If the report has been assigned any other report numbers (*either by the originator or by the sponsor*), also enter this number(s).

10. AVAILABILITY/LIMITATION NOTICES: Enter any limitations on further dissemination of the report, other than those imposed by security classification, using standard statements such as:

(1) "Qualified requesters may obtain copies of this report from DDC."

(2) "Foreign announcement and dissemination of this report by DDC is not authorized."

(3) "U. S. Government agencies may obtain copies of this report directly from DDC. Other qualified DDC users shall request through ________________."

(4) "U. S. military agencies may obtain copies of this report directly from DDC. Other qualified users shall request through ________________."

(5) "All distribution of this report is controlled. Qualified DDC users shall request through ________________."

If the report has been furnished to the Office of Technical Services, Department of Commerce, for sale to the public, indicate this fact and enter the price, if known.

11. SUPPLEMENTARY NOTES: Use for additional explanatory notes.

12. SPONSORING MILITARY ACTIVITY: Enter the name of the departmental project office or laboratory sponsoring (*paying for*) the research and development. Include address.

13. ABSTRACT: Enter an abstract giving a brief and factual summary of the document indicative of the report, even though it may also appear elsewhere in the body of the technical report. If additional space is required, a continuation sheet shall be attached.

It is highly desirable that the abstract of classified reports be unclassified. Each paragraph of the abstract shall end with an indication of the military security classification of the information in the paragraph, represented as *(TS)*, *(S)*, *(C)*, or *(U)*.

There is no limitation on the length of the abstract. However, the suggested length is from 150 to 225 words.

14. KEY WORDS: Key words are technically meaningful terms or short phrases that characterize a report and may be used as index entries for cataloging the report. Key words must be selected so that no security classification is required. Identifiers, such as equipment model designation, trade name, military project code name, geographic location, may be used as key words but will be followed by an indication of technical context. The assignment of links, roles, and weights is optional.

DD FORM 1 JAN 64 1473 (BACK)

Unclassified

Security Classification